NOAA Technical Report NESDIS 65

A NOISE LEVEL ANALYSIS OF SPECIAL MULTIPLE-SPIN VAS DATA DURING STORM-FEST

Washington, D.C.
April 1993

U.S. DEPARTMENT OF COMMERCE
National Oceanic and Atmospheric Administration
National Environmental Satellite, Data, and Information Service

NOAA TECHNICAL REPORTS

National Environmental Satellite, Data, and Information Service

...nvironmental Satellite, Data, and Information Service (NESDIS) manages the Nation's civil Earth-...systems, as well as global national data bases for meteorology, oceanography, geophysics, and solar-...s. From these sources, it develops and disseminates environmental data and information products critical to the protection of life and property, national defence, the national economy, energy development and distribution, global food supplies, and the development of natural resources.

Publication in the NOAA Technical Report series does not preclude later publication in scientific journals in expanded or modified form. The NESDIS series of NOAA Technical Reports is a continuation of the former NESS and EDIS series of NOAA Technical Reports and the NESC and EDS series of Environmental Science Services Administration (ESSA) Technical Reports.

A limited number of copies are available by contacting Nancy Everson, NOAA/NESDIS, E/RA22, 5200 Auth Road, Washington D.C., 20233. Copies can also be ordered from the National Technical Information Service (NTIS), U.S. Department of Commerce, Sills Bldg., 5285 Port Royal Road, Springfield, VA. 22161, (703) 487-4650 (prices on request for paper copies or microfiche, please refer to PB number when ordering). A partial listing of more recent reports appear below:

NESDIS 12 Utilization of the Polar Platform of NASA's Space Station Program for Operational Earth Observations. John H. McElroy and Stanley R. Schneider, September 1984. (PB85 1525027/AS)

NESDIS 13 Summary and Analyses of the NOAA N-ROSS/ERS-1 Environmental Data Development Activity. John W. Sherman III, February 1985. (PB85 222743/A3)

NESDIS 14 NOAA N-ROSS/ERS-1 Environmental Data Development (NNEEDD) Activity. John W. Sherman III, February 1985. (PB86 139284/AS)

NESDIS 15 NOAA N-ROSS/ERS-1 Environmental Data Development (NNEEDD) Products and Services. Franklin E. Kniskern, February 1985. (PB86 213527/AS)

NESDIS 16 Temporal and Spatial Analyses of Civil Marine Satellite Requirements. Nancy J. Hooper and John W. Sherman III, February 1985 (PB86 212123/AS)

NESDIS 18 Earth Observations and the Polar Platform. John H. McElroy and Stanley R. Schneider, January 1985. (PB85 177624/AS)

NESDIS 19 The Space Station Polar Platform: Intergrating Research and Operational Missions. John H. McElroy and Stanley R. Schneider, January 1985. (PB85 195279/AS)

NESDIS 20 An Atlas of High Altitude Aircraft Measured Radiance of White Sands, New Mexico, in the 450-1050 nm Band. Gilbert R. Smith, Robert H. Levin and John S. Knoll, April 1985. (PB85 204501/AS)

NESDIS 21 High Altitude Measured Radiancè of White Sands, New Mexico, in the 400-2000nm Band Using a Filter Wedge Spectrometer. Gilbert R. Smith and Robert H. Levin, April 1985. (PB85 206084/AS)

NESDIS 22 The Space Station Polar Platform: NOAA Systems Considerations and Requirements. John H. McElroy and Stanley R. Schneider, June 1985. (PB86 6109246/AS)

NESDIS 23 The Use of TOMS Data in Evaluating and Improving the Total Ozone from TOVS Measurements. James H. Lienesch and Prabhat K. K. Pandey, July 1985. (PB86 108412/AS)

NESDIS 24 Satellite-Derived Moisture Profiles. Andrew Timchalk, April 1986. (PB86 232923/AS)

NESDIS 26 Monthly and Seasonal Mean Outgoing Longwave Radiation and Anomalies. Aronold Gruber, Marylin Varnadore, Phillip A. Arkin and Jay S. Winston, October 1987. (PB87 160545/AS)

NESDIS 27 Esttimation of Broadband Planetary Albedo from Opertional Narrowband Satellite Measurements. James Wydick, April 1987. (PB88 107644/AS)

NESDIS 28 The AVHRR/HIRS Operational Method for Satellite Based Sea Surface Temperature Determination. Charles Walton, March 1987. (PB88 107594/AS)

NESDIS 29 The Complementary Roles of Microwave and Infrared Instruments in Atmopsheric Soundings. Larry McMillin, February 1987. (PB87 184917/AS)

NESDIS 30 Planning for Future Generational Sensors and Other Priorities. James C. Fischer, June 1987. (PB87 220802/AS)

NOAA Technical Report NESDIS 65

A NOISE LEVEL ANALYSIS OF SPECIAL MULTIPLE-SPIN VAS DATA DURING STORM-FEST

Donald W. Hillger
James F.W. Purdom
Office of Research and Applications
Regional and Mesoscale Meteorology (RAMM) Branch

and

Debra A. Molenar
Colorado State University
Cooperative Institute for Research in the Atmosphere (CIRA)

Washington, D.C.
April 1993

U.S. DEPARTMENT OF COMMERCE
Ronald H. Brown, Secretary

National Oceanic and Atmospheric Administration
Diana H. Josephson, Acting Under Secretary

National Environmental Satellite, Data, and Information Service
Gregory W. Withee, Acting Assistant Administrator

CONTENTS

Page

LIST OF FIGURES....iv

LIST OF TABLES....iv

ABSTRACT....1

1.0 INTRODUCTION....2

2.0 SPECIAL STORM-FEST VAS DATA....2

2.1 Data file organization....5

3.0 STRUCTURE ANALYSIS....5

3.1 Noise Levels from Structure Analysis....6

3.2 Structure-estimated Noise Levels as a Function of the Number of Spins....8

4.0 REPEAT-VIEW VARIABILITY....8

4.1 Repeat-view Noise Levels as a Function of the Number of Spins....10

5.0 SPACE-LOOK VARIABILITY....11

6.0 COMPARISONS OF NOISE LEVELS TO DESIGN SPECIFICATIONS....13

6.1 Noise Level Comparisons as a Function of the Number of Spins....16

7.0 DIURNAL VARIATIONS IN NOISE LEVELS....16

8.0 SUMMARY AND CONCLUSIONS....27

ACKNOWLEDGEMENTS....29

REFERENCES....30

LIST OF FIGURES

Page

Figure 1....4
Figure 2....7
Figure 3....9
Figure 4....12
Figure 5....14
Figure 6a....17
Figure 6b....18
Figure 6c....19
Figure 6d....20
Figure 6e....21
Figure 6f....22
Figure 6g....23
Figure 6h....24
Figure 6i....25
Figure 6j....26
Figure 7....28

LIST OF TABLES

Page

Table 1....3
Table 2....6
Table 3....10
Table 4....11
Table 5....15
Table 6....27

A NOISE LEVEL ANALYSIS OF SPECIAL MULTIPLE-SPIN VAS DATA DURING STORM-FEST

Donald W. Hillger
James F.W. Purdom

NESDIS, Regional and Mesoscale Meteorology (RAMM) Branch

Debra A. Molenar

Cooperative Institute for Research in the Atmosphere (CIRA)

Colorado State University (CSU)
Fort Collins, CO 80523-0033

ABSTRACT

In December 1989, a special collection period for VAS (VISSR Atmospheric Sounder) data was arranged in order to test the effect of spin budget (multiple samples at the same field-of-view [FOV]) on the noise levels of the VAS channels. Results of that study were reported in NOAA Technical Report 56. However, upon completion of that study, we decided to recalculate some of the results with improvements learned during the first study. Those improvements are: 1) To calculate the results in radiance units instead of effective blackbody temperature units; and, 2) To save VAS data off the edges of the earth to better compare with the space-look noise levels provided by CIMSS. At the same time, some subtle errors in the analysis software have been corrected, resulting in noise levels that now conform to the expected theoretical decrease with increasing numbers of spins.

Special multiple-spin VAS data were available during STORM-FEST (STormscale Operational Research and Meteorology - Fronts Experiment Systems Test) to accomplish these technical improvements. Like the old study, this new study compares noise levels of the VAS channels determined by three methods to the design specifications for the VAS instrument. Results from the three analysis methods agree in general, and results conform to design specification as well, but with some differences. The agreements indicate that all three noise level estimating methods are viable, but the differences indicate that the three methods for determining noise levels should occasionally be intercompared using operational data sets.

Finally noise levels were calculated as a function of time of day, to determine if there was any systematic diurnal variation that can be determined. Results indicate that there was no detectable diurnal variation in noise level of any of the VAS channels.

Noise levels should be determined frequently for any operational data set. For VAS the requirements for sounding errors can then be used to specify the spin budget (number of temporal samples) or the spatial averaging needed to meet those requirements. In the case of GOES-Next, the FOV dwell time may be increased or decreased to alter noise levels. The change in noise level with dwell time should be an ongoing test applied to operational data from GOES-Next.

1.0 INTRODUCTION

High-resolution VISSR Atmospheric Sounder (VAS) radiances with a spin budget of up to 31 spins per channel were taken during a special data collection period from February through mid-March 1992. The purpose of this special collection was to provide data for the STormscale Operational Research and Meteorology - Fronts Experiment Systems Test (STORM-FEST). Although the purpose of STORM-FEST was to look at weather fronts, the opportunity was available to do high-spin-budget noise level determinations.

Noise levels for this special VAS data were determined using three methods. The three methods were: 1) structure function analysis of measurements at adjacent fields-of-view (FOVs); 2) variability of multiple samples (spins) at each FOV; and 3) variability of space-look measurements (provided by CIMSS).

Structure function analysis is a proven technique that allows the determination of noise levels using routine, but cloud-free data. A computer-intensive statistical analysis of the data is used to determine the structure of the data, which is a combination of the spatial gradient and the noise within the data. By removing the spatial gradient from the structure function, the remainder is equivalent to the relative noise determined from calibration measurements. (Hillger and Vonder Haar, 1988).

The statistical variability of multiple measurements at each FOV can also be used to determine the noise level of the data. Since the individual measurements from multiple spins are not saved in operational data sets, this method is only possible using special data collection software which saves the individual measurements at each FOV. Such single-spin data were collected at CIRA for this repeat-view analysis.

Finally, noise level results from analysis of space-look measurements were provided by Mr. T.J. Schmit of NESDIS/CIMSS (Cooperative Institute for Meteorological Satellite Studies). The variability of these no-spatial-gradient (off-the-earth) measurements should be equal to the noise level of the instrument. Such space-look measurements are used by CIMSS to occasionally determine the noise levels of operational data.

Plots of noise levels versus the number of spins for each VAS channel will be shown. Noise levels derived from structure function analysis will be compared to the statistical variability of multiple measurements at each FOV and compared to space-look noise level estimates. Then all three methods will be compared to the VAS design specifications.

2.0 SPECIAL STORM-FEST VAS DATA

Special VAS software was used to collect the individual-spin (single-sample) radiance measurements during STORM-FEST for February through mid-March 1992. The highest-spin-budget schemes for data collection were called Meso-Beta. During the 10-minute Meso-Beta schedule, VAS data were collected only over a limited north-south span over the STORM-FEST region but for the full-width of the earth. Each VAS channel was sampled a minimum of 9 times, with the exception of

VAS window channels 8 and 12 which were sampled only once for each channel. Data were collected by the CIRA ground station every 6 hours (4 times per day) during normal operations and as frequently as possible during Intensive Operations Period (IOP) days. Table 1 provides some basic information about the VAS channels for the 10-minute Meso-Beta schedule. This table can be used for reference regarding VAS channel characteristics. For example, column 4 gives the approximate peak weighting level for each of the VAS channels.

Table 1

VAS Channel Information for 10-minute Meso-Beta schedule

VAS Channel	Filter Center (μm)	Effective Wavenumber (cm^{-1})	Approximate Peak Weight Level (hPa)	Horizontal Resolution (km)	Number of Spins
1	14.7	680	70	16	20
2	14.5	690	125	16	9
3	14.3	700	200	8	21
4	14.0	715	500	8	10
5	13.3	750	920	8	16
6	4.5	2208	850	16	9
7	12.7	789	1000	8	20
8	11.2	897	surface	16	1
9	7.3	1375	600	8	31
10	6.8	1486	400	8	14
11	4.4	2253	300	16	13
12	3.9	2541	surface	16	1

Data were collected for a total of either 7 or 10 different scan lines (depending on the FOV size) that covered the entire width of a full-disk earth image. After finding very few areas on the earth with spatially homogeneous non-cloudy radiances for noise level determination, we decided to use VAS radiances from off the edge of the earth. Of this off-the-earth data an area of 100 along-line FOVs from each of the 7 or 10 scan lines was chosen for intensive analysis. Data for all VAS channels were taken at the horizontal resolution as shown in column 5 of Table 1. For small-FOV sensors up to 10 scan lines of VAS data were available, whereas for large-FOV sensors only 7 scan lines of VAS data were available. The line-to-line spacing changes between the small-FOV sensors and the large-FOV sensors. For both FOV sizes, the along-line spacing is equal (8 km at nadir).

Figure 1 shows a sample of VAS radiances from off the western edge of the earth for 1848 UTC on 20 February 1992. (This is the date and time used for all testing except the diurnal variation studies performed at CIRA.) The first 500 FOVs are shown for VAS channel 1, which has a large noise level and a low signal-to-noise ratio. The signal from space is basically random, although subjectively there may appear to be a trend in this data for spin-1 and scan-line-1 on this day. This figure contains only a sample of the larger statistical base of VAS data used in this noise level analysis. There appears to be no correlation between the radiances in Figure 1 and those for other spins and other scan lines (not shown), as should be expected.

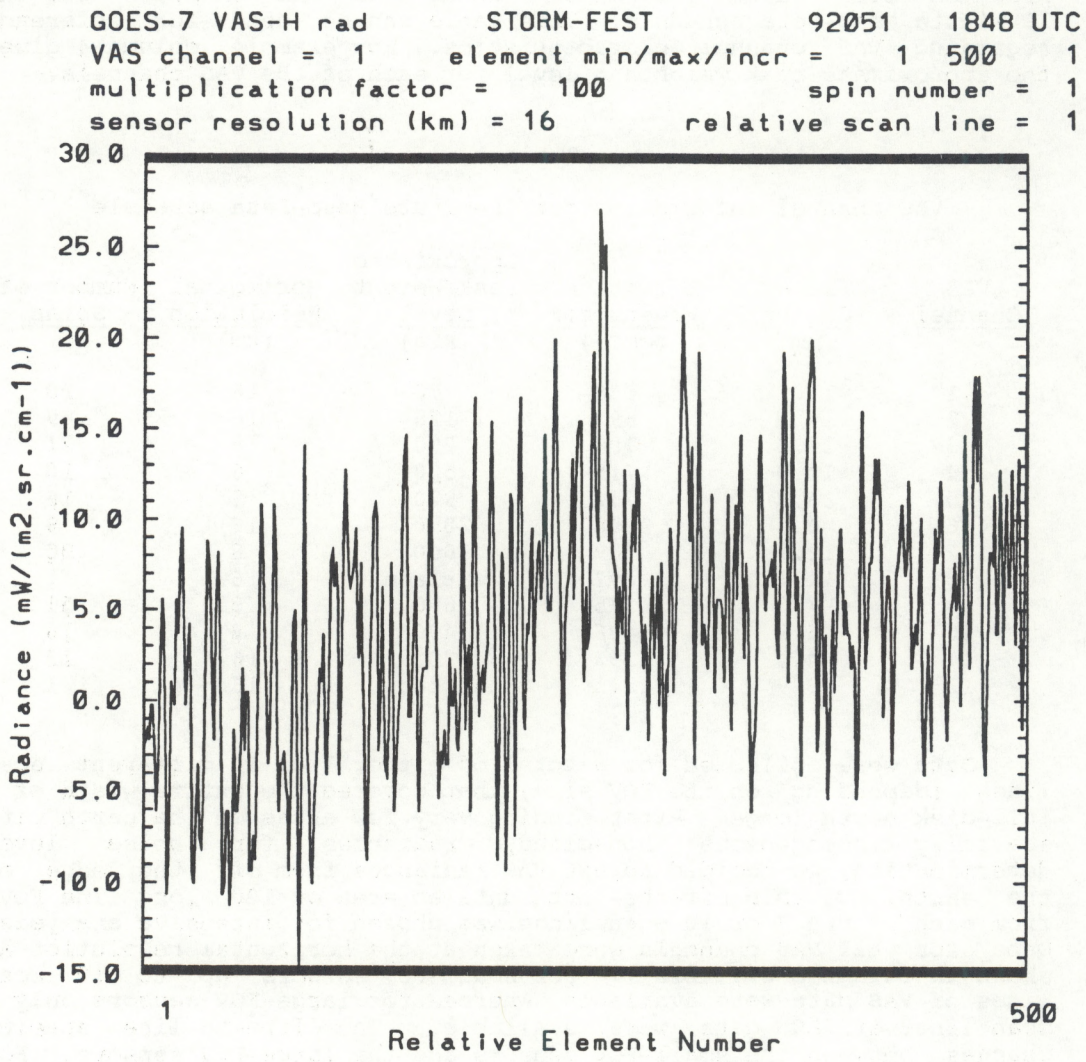

Figure 1: VAS channel 1 signal composed entirely of noise from off the edge of the earth. The first 500 elements are shown for spin-1 and scan-line-1 prior to viewing the western edge of the earth.

2.1 Data file organization

VAS data were organized into two different file types in order to compute the necessary statistics. After first being saved in one huge dwell-sounding file, software was used to separate the data stream into a file for each sensor size and spin. Up to 31 single-sample (1-spin) files were created for each VAS channel. The 6 small-FOV channels and the 6 large-FOV channels were put into separate files. The reason for this was to simultaneously compute statistics on VAS channels with equal line-to-line spacing. These single-spin data files were used to compute the repeat-view statistics. Additional software was used to produce spin-averaged radiance files from the single-spin radiance files. This resulted in up to 31 files for each channel. These spin-averaged radiances were used to compute the structure-estimated noise levels.

In the original data stream the various channels and spins are transmitted in a mixed (non-consecutive) order. That mixed order is based on the arrangement of the infrared filters and upon a paired arrangement of sensors in the VAS instrument. At the time of separation into data files for each spin, the VAS data were reorganized into a form where scan lines are consecutive and VAS channels are separated. A file with consecutive scan lines can be displayed as an image. Conversion from measured count values to radiances and navigation of the data take place at the time of separation into individual files.

3.0 STRUCTURE ANALYSIS

One method of determining the noise level of satellite measurements is by structure function analysis (Hillger and Vonder Haar, 1979, and 1988; Wald, 1989) Structure analysis statistically compares measurements at adjacent FOVs to determine the gradient as a function of separation distance (Gomis and Alonso, 1988). The structure function is then objectively extrapolated to zero separation distance, effectively taking the spatial gradient out of the statistics. The remaining structure at zero distance can be shown to be twice the noise variance (the square of the standard error [e]) (Gandin, 1963),

$$\text{structure at zero separation distance} = 2e^2 . \qquad (1)$$

Examples of structure function plots were given in NOAA Technical Report 56 (Hillger et al, 1991). The structure function was computed by comparing only those measurements from one scan line to the next scan line. Adjacent measurements on different scan lines should be entirely independent of sensor response, whereas adjacent measurements along the same scan line are correlated because the VAS sensor's response is slower than its sampling frequency (the measurements are convolved). (For details on convolution of the VAS infrared signal, see Gabriel and Purdom [1990a and b].) Structure analysis of the along-line measurements, because the measurements are correlated, underestimates the true spatial gradient (and the estimated noise) between nearby measurements. Thus, the results from along-line statistics are not useful for noise level estimation, and only the line-to-line statistics are used in this study.

3.1 Noise Levels from Structure Analysis

Structure function analysis was run on each of the spin-averaged VAS radiance files for 1 to 31 spins per channel. Single-spin (1-spin-per-channel) results for each of the 12 VAS channels are given in Table 2. Column 2 of Table 2 gives the multiplication factor applied to each VAS channel. This factor was determined in order to make the signal and noise radiances of similar magnitude among the VAS channels. For some channels the multiplication factor is 1, indicating that the radiances are actual values, whereas for other channels the multiplication factors are either 10 or 100, indicating that the radiances have been increased by that factor.

Table 2

Single-sample (1-spin) Structure-estimated Noise Levels
Date: 1992-February-20 (Julian-day 51)

VAS Channel	Mult-Factor	Signal Level (mW/...)	Maximum RMS Noise (mW/...)	Minimum RMS Noise (mW/...)	Signal-to-Noise
1	1	21.8	4.97	4.97	4.4
2	1	20.4	2.43	2.43	8.4
3	1	20.4	2.49	2.33	8.2
4	1	23.3	1.78	1.78	13.1
5	1	31.8	1.68	1.44	18.9
6	100	16.1	4.07	4.07	4.0
7	1	38.1	1.35	1.35	28.2
8	1	33.5	0.15	0.15	223.
9	10	49.7	13.35	13.21	3.7
10	10	20.13	3.39	3.39	5.9
11	100	9.91	4.43	4.43	2.2
12	100	29.4	1.12	1.12	26.2

radiance units (mW/[m^2 sr cm^{-1}])

Column 3 of Table 2 gives the signal level found in each VAS channel. This is the standard deviation of the radiances observed over the earth for the day being analyzed. Columns 4 and 5 give the maximum and the minimum structure-estimated noise levels. The maximum noise level is from the un-extrapolated structure and the minimum noise level is from the structure objectively extrapolated to zero separation distance. These two noise levels are often similar since no spatial gradient exists in the off-the-earth (space) measurements. Finally, the last column of Table 2 gives the signal-to-noise ratio for each VAS channel. These numbers are the ratios of the signal (column 3) to the maximum structure-estimated noise level (column 4).

Figure 2 gives the noise levels for each of the 12 VAS channels (the same numbers as in Table 2) in graphical form. Similar figures were generated for 1 to 31 spins, but only the single-sample (1-spin-per-channel) case is shown. Values of signal level and noise level, referred to below, are in radiance units (mW/[m^2 sr cm^{-1}]). The longest vertical bar for each VAS channel is the signal, which is simply the standard deviation of all the measurements that were collected at the time of analysis, indicating the natural variability of the weather seen in each of the VAS channels. Two estimates of the

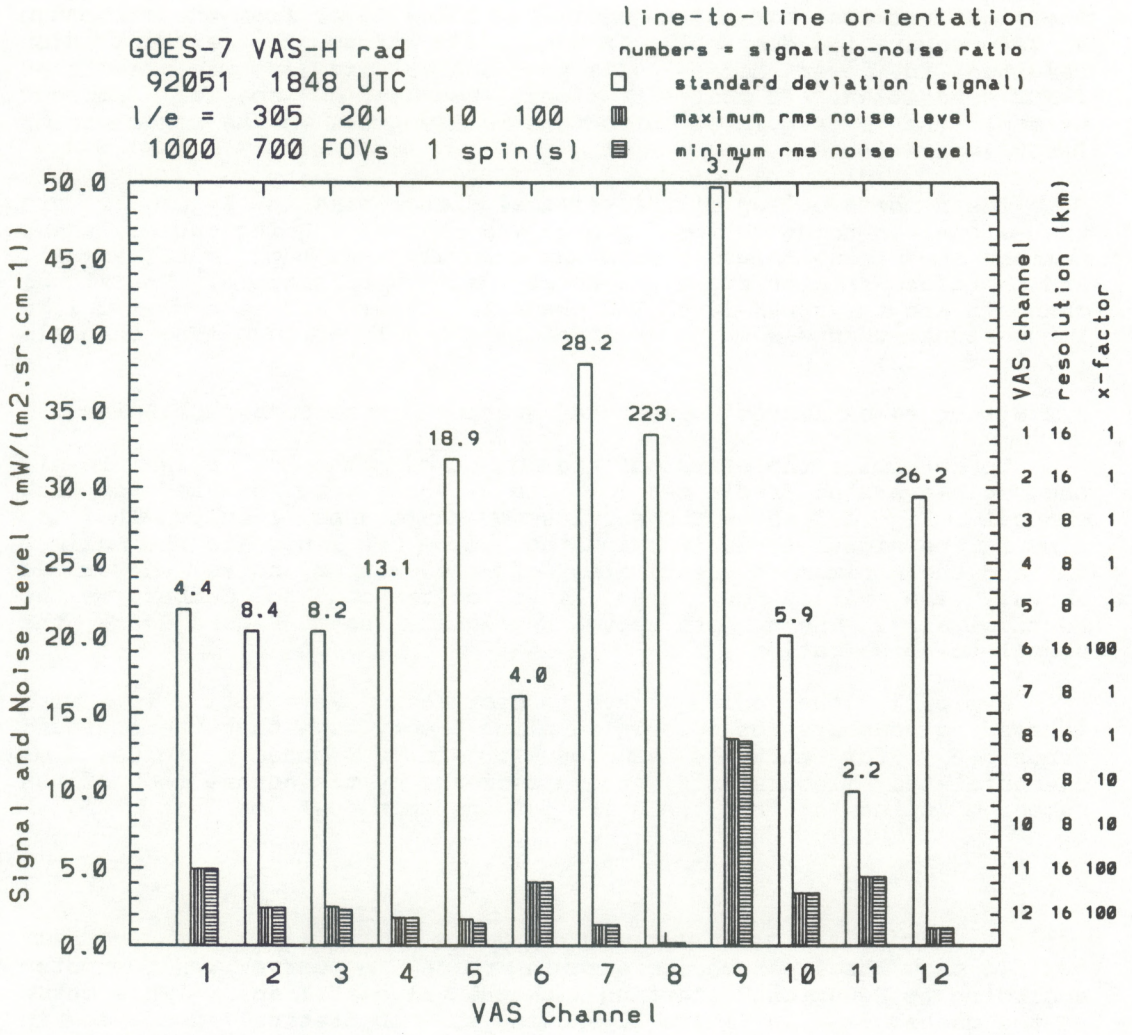

Figure 2: Single-sample (1-spin-per-channel) structure-estimated noise levels for each of the 12 VAS channels. For each channel the longest vertical bar is signal, the two shorter vertical bars (see legend) are the maximum and the minimum noise level estimates. Numbers on top of the vertical signal bars are dimensionless signal-to-noise ratios. Statistics are computed in the preferred line-to-line orientation to avoid along-line correlations due to sensor response. Also, note that the multiplication-factors (x-factors) applied to the radiances in each VAS channel can vary.

noise level are given. The left of the two shorter vertical bars is the noise level from the structure at 1-FOV separation. This structure at non-zero distance may contain spatial gradient information and therefore may overestimate the actual noise level. The right vertical bar is the estimated noise level from the structure at zero separation distance. In some situations the extrapolation resulted in lower noise levels when spatial gradient was present at 1-FOV separation. In most situations (because no spatial gradient exists) the extrapolated structure is identical to the structure at 1-FOV separation.

The numbers on top of the vertical signal bars in Figure 2 are the signal-to-noise ratios for each VAS channel. Being ratios, these numbers are dimensionless. Some VAS channels have much more signal, and therefore greater signal-to-noise than other channels. Low signal channels are the upper-level VAS channels (1-3) and others, unlike large-signal channels which are typically the lower-level VAS channels (7, 8, and 12).

3.2 Structure-estimated Noise as a Function of the Number of Spins

To determine the effect of the number of spins on noise level, the spin-averaged radiances for 1 to 31 spins were analyzed for each channel. Figure 3 shows the results for VAS channel 1 only. The top line is the signal level 'S', and the bottom two lines are the maximum 'X' and the minimum 'N' estimates of the random noise, described above. The values on these lines correspond to numbers on the vertical axis. The numbers above the signal line in Figure 3 are the signal-to-noise ratios.

Typically the noise level decreases asymptotically with increasing numbers of spins. Sampling theory says that the standard error (e_n) for multiple samples (or in our case, spins) of un-correlated measurements should decrease by the square root of the number of spins (n) from the noise for one spin (e_1), or

$$e_n = e_1 / n^{1/2} . \qquad (2)$$

To show the expected decrease in noise, a curve was computed according to Equation 2 starting with the value at 1 spin. This curve is the dashed line in Figure 3, showing the theoretical decrease in noise level with increasing numbers of spins. For nearly all VAS channels the decrease in structure-estimated noise with increasing numbers of spins follows the shape of the theoretical curve. A few exceptions include the minimum noise levels for some VAS channels, where the extrapolations to zero separation distance appear to be invalid. These exceptions will be apparent when the structure-estimated results are compared to the other noise level methods.

4.0 REPEAT-VIEW VARIABILITY

Besides the structure analysis, another measure of the noise levels of the VAS channels was obtained by statistically comparing the variability of multiple measurements over the same FOVs. This method is not possible with operational data, because the individual

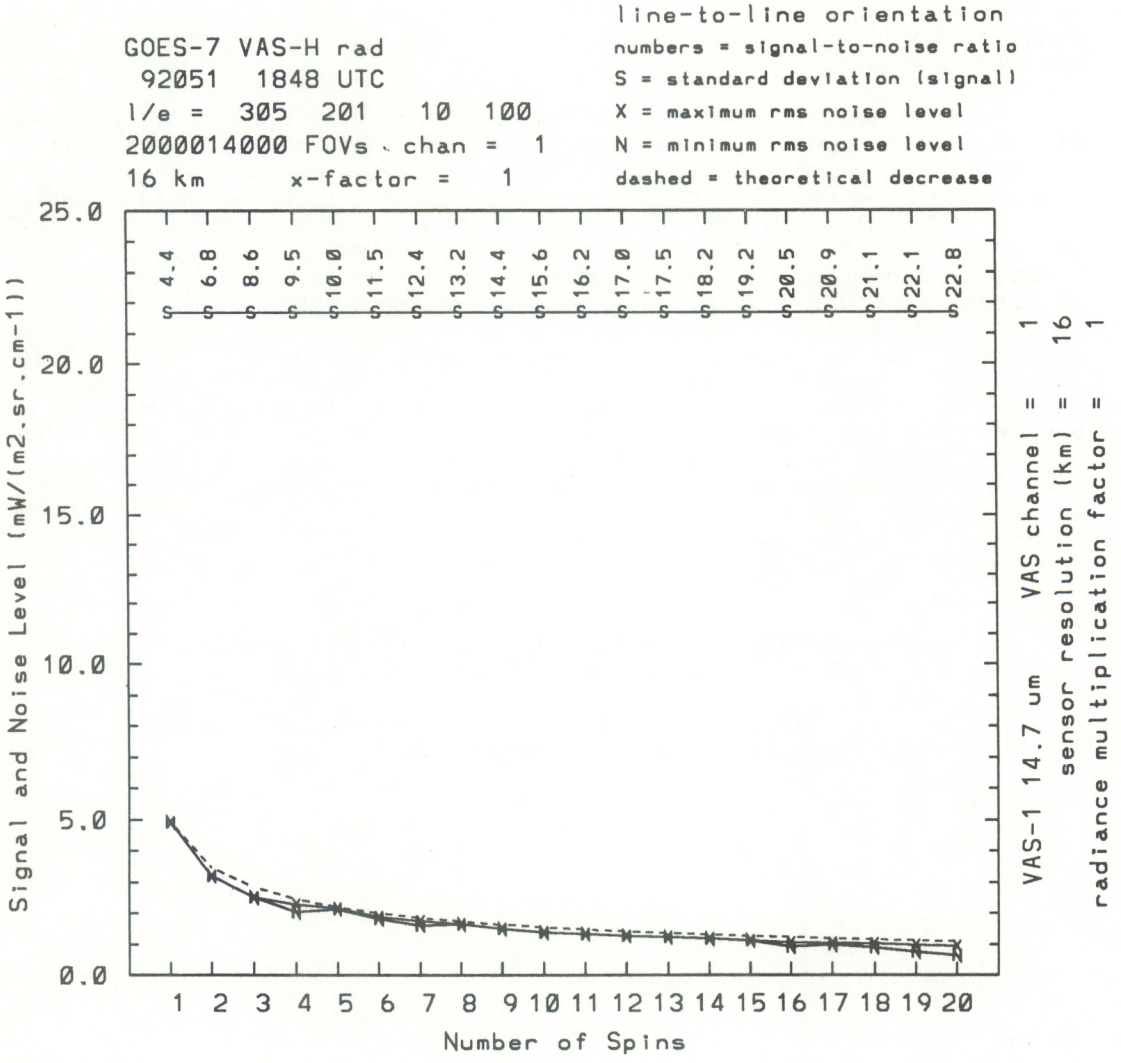

Figure 3: Structure-estimated noise level as a function of the number of spins for VAS channel 1. Labeling of lines ('S','X', and 'N') is explained in the text and in the legend on top. The dashed line is the theoretical decrease in noise level with increasing numbers of spins (samples). The values on all lines correspond to the numbers on the vertical axis. The numbers above the signal line are dimensionless signal-to-noise ratios for each VAS channel. Measurements from adjacent FOVs are statistically compared in the line-to-line orientation.

measurements for each spin are not normally saved, but are immediately summed and later averaged to give a single value for each FOV. However for this special data set, the individual measurements for each spin were saved in single-spin files and were statistically analyzed to determine the variability of the measurements in each of the VAS channels.

Because multiple samples (spins) were taken at each FOV, it is possible to compute the standard deviation of the individual samples. The resulting statistic is called the repeat-view variability since it represents the variability of the single-sample (1-spin) measurements at any FOV. Also, by adding together groups of, for example, 2 spins at a time, it is possible to compute the variability of up to 15 independent samples of 2-spin averaged measurements, as in the case of 31 spins for VAS channel 9. For other channels the number of 2-spin combinations is fewer. Likewise if 3 spins at a time are averaged together, it is possible to compute the variability of up to 10 independent samples of 3-spin averaged measurements, as in the case of 31 spins. However, it is not possible to form more independent samples than half the number of available spins for any given VAS channel. The maximum number of spins for which a minimum of 2 independent samples are available for repeat-view statistics is given in column 2 of Table 3.

Table 3

Single-sample (1-spin) Repeat-view Noise Levels
Date: 1992-February-20 (Julian-day 51)

VAS Channel	Maximum Spins	Mult-Factor	Repeat-view Variability (mW/...)
1	10	1	4.84
2	4	1	2.30
3	10	1	2.66
4	5	1	1.74
5	8	1	1.75
6	4	100	3.99
7	10	1	1.41
8	1	1	0.14
9	15	10	13.32
10	7	10	3.38
11	6	100	4.68
12	1	100	1.05

radiance units ($mW/[m^2\ sr\ cm^{-1}]$)

Column 3 of Table 3 gives the multiplication factor for the noise levels, and column 4 gives the repeat-view noise level for each of the VAS channels. Only single-spin noise levels are given. Results of computations at other number of spins are given below.

4.1 Repeat-view Noise Levels as a Function of the Number of Spins

As expected, there is a decrease in noise level with increasing numbers of spins (samples), as was the case for the structure analysis. The repeat-view noise levels for VAS channel 1 are plotted

in Figure 4. The line labeled 'R' is the repeat-view noise computed for up to 10 spins (out of the 20 available spins for VAS channel 1). For comparison purposes the theoretical decrease in noise with increasing numbers of spins is plotted as an dashed line in Figure 4. The theoretical curve starts with the value for 1 spin and uses Equation 2 to compute the values for multiple spins. For all VAS channels the measured and theoretical curves are similar, as will be show below, indicating that the noise levels do decrease as expected by theory.

5.0 SPACE-LOOK VARIABILITY

During this special STORM-FEST period, NESDIS/CIMSS computed the variability of space-look (well off the edge of the earth) measurements (Schmit, 1992; Schmit and Menzel, 1992). Table 4 lists the space-look results for 2048 UTC on 20 February 1992. (This is 2 hours later than the time of the data set used for the previous results.) For each VAS channel the maximum number of spins is given in column 2. For all VAS channels, the space-look variability in column 3 was measured as the standard deviation of about 450 multiple-spin averaged measurements. Because multiple spins were collected, the average variability in column 3 is reduced from the expected single-spin noise. These numbers were then converted into single-sample (1-spin) noise levels in column 4 using the inverse of Equation 2. This is the single-spin noise assuming that noise increases as the square root of the number of spins decreases. Column 3 contains measured values, whereas column 4 contains derived values. All noise levels are given in radiance units (mW/[m^2 sr cm^{-1}]). The resulting space-look noise levels are compared below to both the structure-estimated noise levels and the repeat-view variabilities.

Table 4

Space-look Noise Levels
Date: 1992-February-20 (Julian-day 51)

VAS Channel	Number of Spins	Space-look Variability (mW/...)	Single-sample Variability (mW/...)	Digitization Level (mW/...)
1	20	1.04	4.65	0.12
2	9	0.64	1.92	0.14
3	21	0.50	2.29	0.15
4	10	0.42	1.33	0.17
5	16	0.37	1.48	0.24
6	9	0.009	0.027	0.0025
7	20	0.31	1.39	0.26
8	1	0.13	0.13	0.24
9	31	0.17	0.95	0.04
10	14	0.07	0.26	0.02
11	13	0.01	0.036	0.0025
12	1	0.006	0.006	0.0025

radiance units (mW/[m^2 sr cm^{-1}])

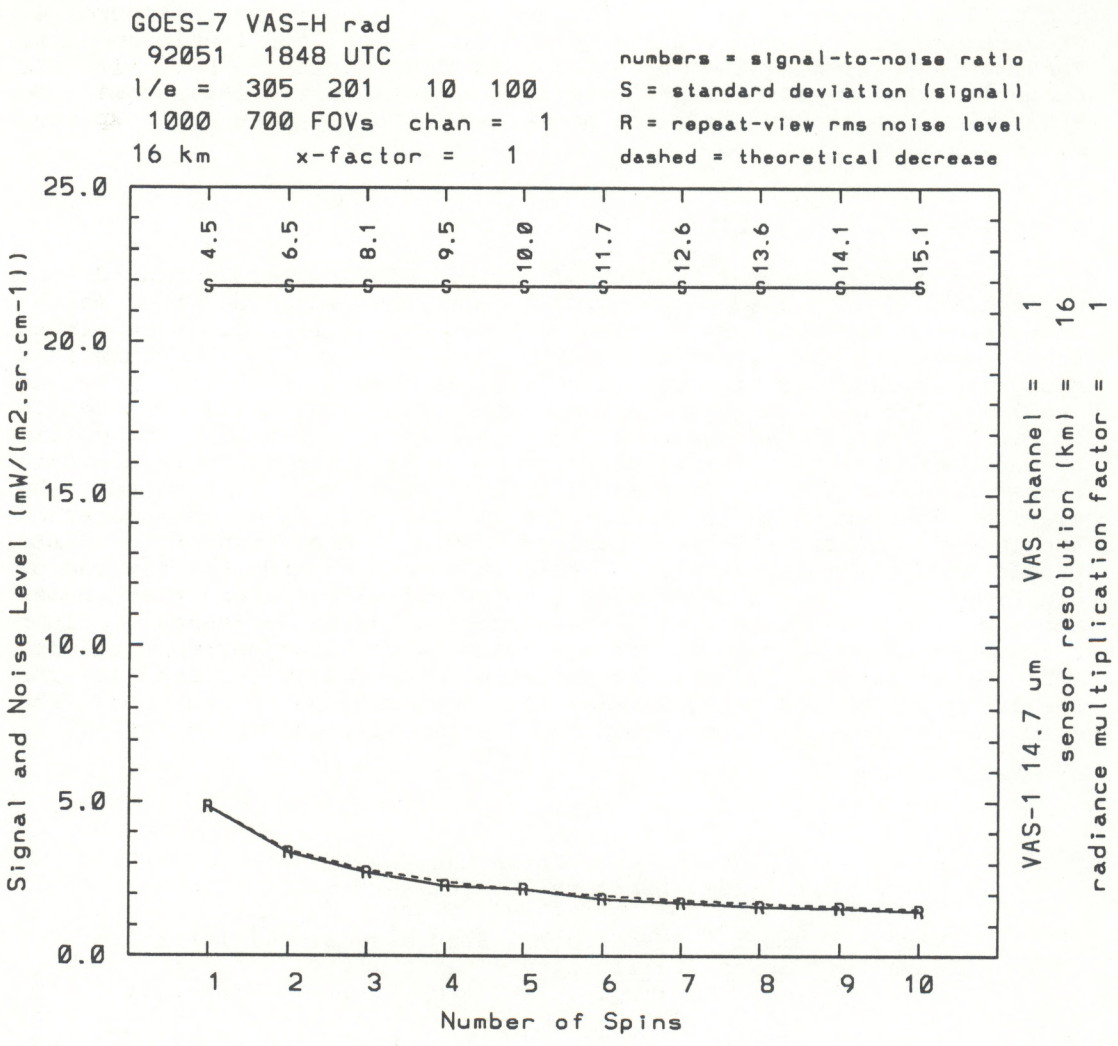

Figure 4: Repeat-view noise level as a function of the number of spins for VAS channel 1. The line labeled 'R' is the noise level for 1 through 10 spins (the maximum possible number of spins in 2 independent samples out of 20 total spins). The dashed line is the theoretical decrease in noise level with increasing numbers of spins (samples).

Finally, the last column of Table 4 gives the digitization level for each of the VAS channels. This is the radiance difference between each count value from the VAS instrument, depending on the channel being considered. Of all the VAS channels, only the noise level in VAS channel 8 in columns 3 or 4 (0.13 mW/[m^2 sr cm^{-1}]) approaches the digitization level of the satellite radiances for this channel. For VAS channel 8 the digitization level for 1 measured count value is about 0.24 mW/(m^2 sr cm^{-1}), which means that radiances cannot be determined within plus or minus one half (0.12 mW/[m^2 sr cm^{-1}]) of the radiance digitization level. This digitation level is also close to the structure-estimated noise level at 1 spin (0.15 mW/[m^2 sr cm^{-1}]) in columns 4 or 5 of Table 2. A true noise level less than the digitization level cannot be determined, since the digitization level limits the precision of the measured radiances. This may indicate that the measurements in VAS channel 8 alone are digitization limited. Only with a lower digitization level between count values can the VAS channel 8 noise level be determined.

6.0 COMPARISONS OF NOISE LEVELS TO DESIGN SPECIFICATIONS

The noise levels estimated by performing structure function analysis and computed from repeat-view statistics should be similar to those obtained from space-look data. Table 5 is a comparison of noise levels from these three analysis methods. Column 3 gives the structure-estimated noise level, column 4 gives the repeat-view variability, and column 5 gives the space-look variability (from column 4 of Table 4). In addition, the last column in Table 5 gives the pre-launch design specification for single-sample VAS measurements (Chesters and Robinson, 1983; Chesters et al, 1985). In each column the noise levels are for single-sample (1-spin) measurements.

Figure 5 is a bar graph of the single-sample noise levels from Table 5. Vertical bars with different shading are used to compare the three noise level determinations to the pre-launch design specifications for each VAS channel. Maximum structure-estimated noise levels are unshaded. Repeat-view noise levels are shaded with vertical lines. Space-look noise levels are shaded with horizontal lines. The design specifications are shaded black.

The structure-estimated noise levels compare well with the repeat-view variability for all channels. By using off-the-earth radiances with no spatial gradient, problems with extrapolating the structure function to zero distance have been largely eliminated. Such problems were common to VAS channels 8 and 12 in the previous study (Hillger et al, 1991). The problem was the inability to remove all of the spatial gradient information from the structure analysis. For the VAS window channels (8 and 12) there is often great variability at small scales, even below the resolution of the VAS instrument. It is hard to effectively eliminate (extrapolate out) all the spatial gradient from such highly variable channels. By employing off-the-earth radiances with no gradient the structure-estimated noise levels are more reliable.

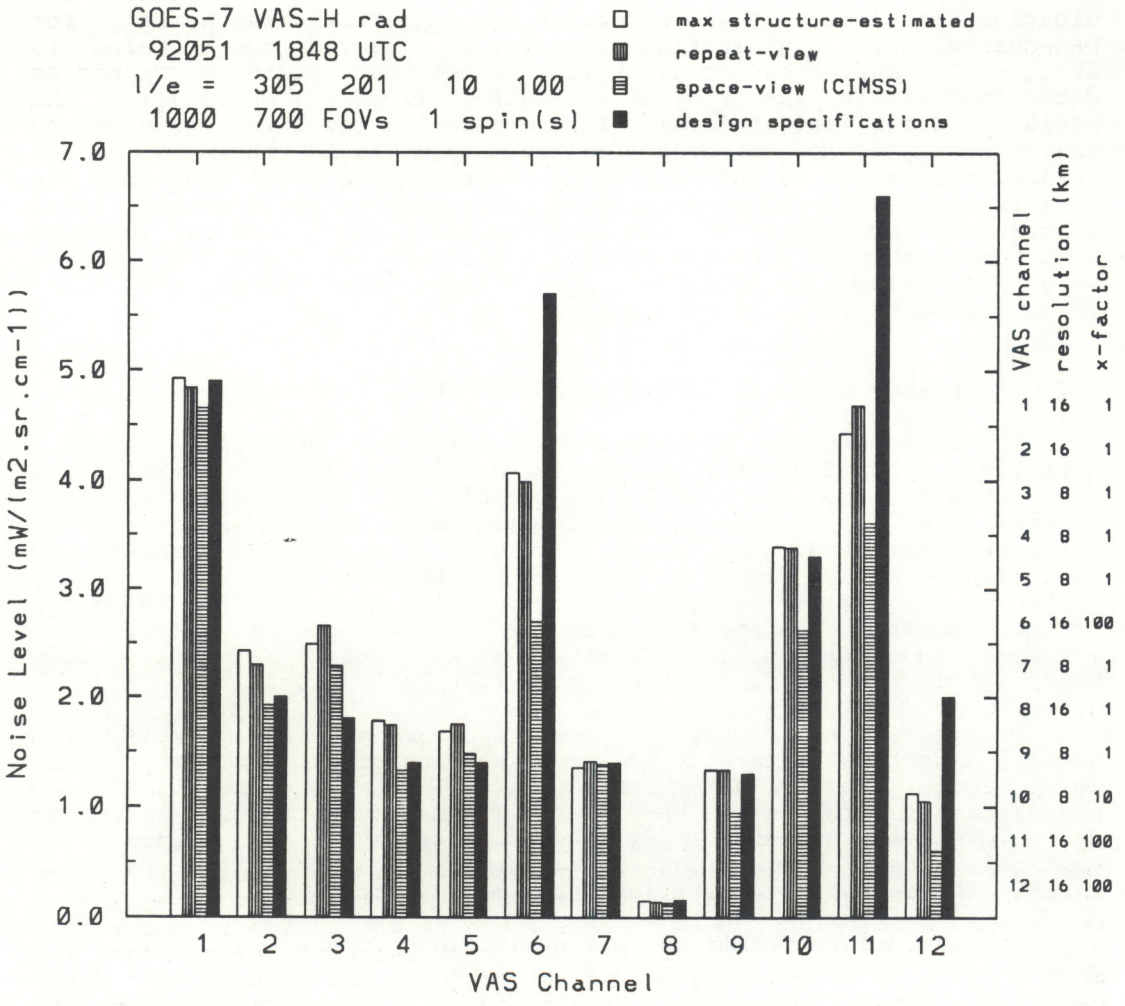

Figure 5: Single-sample (1-spin) noise levels from the three different analysis methods compared to the pre-launch design specifications for each of the 12 VAS channels. The numbers are the same as in Table 5. Vertical bars with different shading (see the legend) are used for each analysis method.

Table 5

Single-sample (1-spin) Noise Level Comparison
Date: 1992-February-20 (Julian-day 51)

VAS Channel	Mult-Factor	Structure* -estimate (mW/...)	Repeat-view** Variability (mW/...)	Space-look*** Variability (mW/...)	Single-sample Design Specs (mW/...)
1	1	4.97	4.84	4.65	4.9
2	1	2.43	2.30	1.92	2.0
3	1	2.49	2.66	2.29	1.8
4	1	1.78	1.74	1.33	1.4
5	1	1.68	1.75	1.48	1.4
6	100	4.07	3.99	2.7	5.7
7	1	1.35	1.41	1.39	1.4
8	1	0.15	0.14	0.12	0.16
9	1	13.35	13.32	9.5	13.
10	10	3.39	3.38	2.6	3.3
11	100	4.43	4.68	3.6	6.6
12	100	1.12	1.05	0.7	2.0

radiance units (mW/[m^2 sr cm^{-1}])

* from Table 2, column 4
** from Table 3, column 4
*** from Table 4, column 4

Next, the structure-estimated and repeat-view noise levels are compared to single-sample (1-spin) space-look noise level in column 5 of Table 5 (from column 4 of Table 4). For most channels the noise levels differ by very little, except for VAS channels 6, 9, 10, 11, and 12. But for nearly all VAS channels the noise levels as estimated by structure analysis and by repeat-view variability are greater than the space-look variability. This general tendency can be explained by the fact that the space-look results were determined from measurements, some of which are correlated since they are taken from adjacent FOVs along the same scan line. The reduced standard deviation of correlated measurements would result in lower than actual noise levels. In contrast, for the first two methods an effort was made to exclude all correlated measurements. The difference would cause the space-look noise levels to be slightly but consistently lower than noise levels determined by the other two methods. Further testing at CIMSS verified that the inclusion of correlated measurements from the same scan line does have the expected effect upon the space-look noise levels (Schmit, 1993).

Finally, the comparison to the single-sample (1-spin) design specification produces some interesting comparisons. For most VAS channels the three noise level estimates are very similar and they agree with the design specifications. But for VAS channels 6, 11, 12 the estimated noise levels are significantly smaller than the design specifications. This is entirely possible, since the design specifications are usually met, if not exceeded. Interestingly, these are three of the channels where the space-look noise levels differ significantly from the the better agreement between the first two noise level methods, putting some additional doubt into the comparability of the space-look results.

6.1 Noise Level Comparisons as a Function of the Number of Spins

Figures 6a through 6j show comparisons of the noise levels determined by the various analysis methods as a function of the number of spins for each VAS channel. Results are shown for all except VAS channels 8 and 12 where only 1-spin is available for each channel. Results for those channels are already given in Table 5. The letters 'X' and 'N' are used to represent the maximum and the minimum structure-estimated noise levels, 'R' represents the repeat-view results, 'S' gives the space-look results from CIMSS, and 'D' represents the design specifications. The space-look results are determined at the maximum number of spins (same numbers as in column 3 of Table 4) and are converted to other numbers of spins. The design specifications are given at 1 spin (from the last column of Table 5) and are converted to other numbers of spins, thus these two lines exactly follow the theoretical decrease in noise with increasing numbers of spins.

Finally, the dashed line at the bottom of each of Figures 6a through 6j is the radiance digitization level for each channel. This is the radiance increment between consecutive image counts, or the slope (1st-order) coefficient of the linear conversion from image counts to radiances. For each channel the value at 1 spin comes from the last column of Table 4. Values at other numbers of spins are calculated using Equation 2. Half of this value is the minimum level for noise determination, and can be thought of as the uncertainty of the noise estimates.

In nearly all channels the structure-estimated and repeat-view noise levels follow the theoretical decrease expected for increasing numbers of samples (spins). The only exceptions are some of the minimum (or extrapolated) noise levels 'N' where the extrapolation appears to underestimate the true noise level according to theory. This is especially true for VAS channels 1 and 6. For some channels large differences exist between the structure-estimated/repeat-view noise and the space-look results from CIMSS. Note especially VAS channels 6, 10, and 11. If the differences are not due to the inclusion of correlated measurements in the space-look analysis, then it questions the reliability of using any one noise level determination method.

7.0 DIURNAL VARIATIONS IN NOISE LEVELS

To determine if there was any diurnal variation in noise in the course of a day, the single-spin repeat-view noise levels were calculated every 3 hours from 1447 UTC on Julian-day 66 (1992-March-06) to 1750 UTC on Julian-day 67 (1992-March-07) during one of the Intensive Operation Periods. This time span covers 10 times for a total of 30 hours. Some overlap in time span was purposely included. Results for all 12 VAS channels are shown in Table 6. Column 2 gives the multiplication factor for each radiance, column 3 gives the average noise level, column 4 gives the noise level standard deviation, and the last column gives the percentage of the noise standard deviation compared to the average noise. For most channels the noise varied by only a few percent, except for VAS channel 8. The conclusion is that the variability with time is very low and is probably not significant.

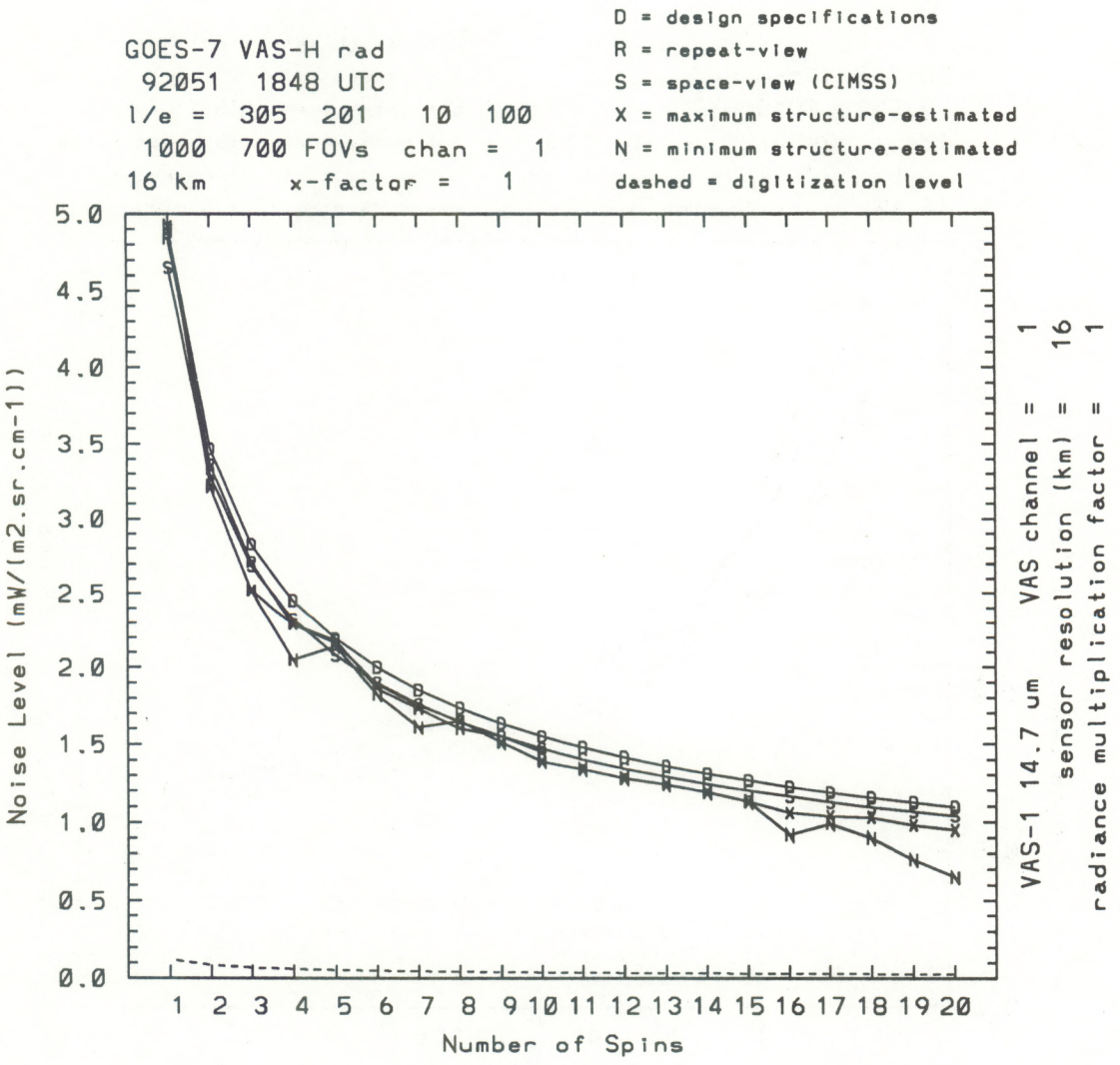

Figure 6a: Noise levels for VAS channel 1 from the three different analysis methods compared to the pre-launch design specifications as a function of the number of spins. Lines are labeled according to the legend on top. Only the structure-estimated and repeat-view noise levels are computed independently for different numbers of spins. The space-look (CIMSS) noise levels were computed at the maximum number of spins and were converted to lesser numbers of spins by using noise level theory. The design specifications are given for one spin and were converted to multiple numbers of spins using noise level theory. The dashed line is the radiance digitization level for this channel.

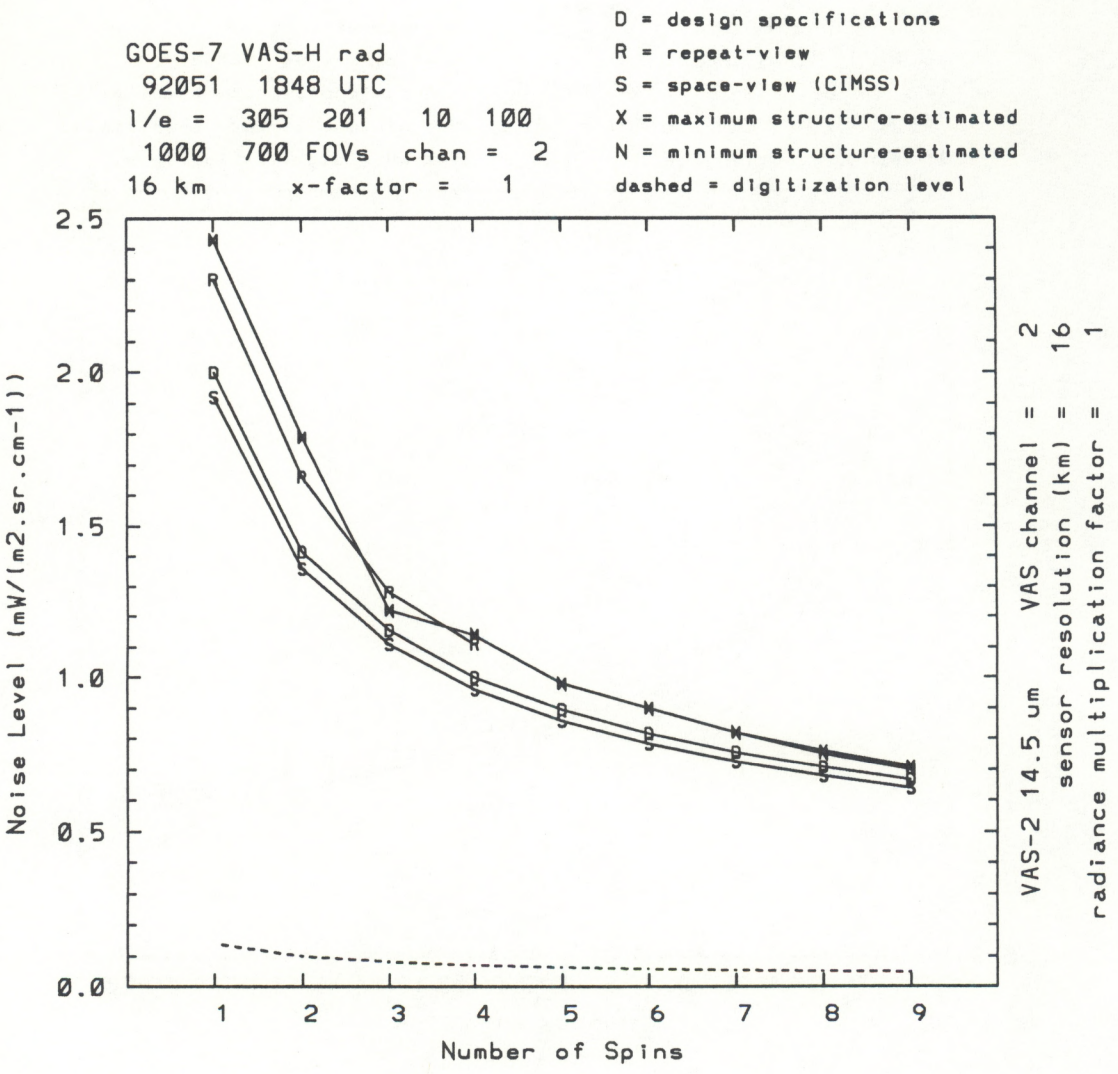

Figure 6b: Same as Figure 6a, but for VAS channel 2.

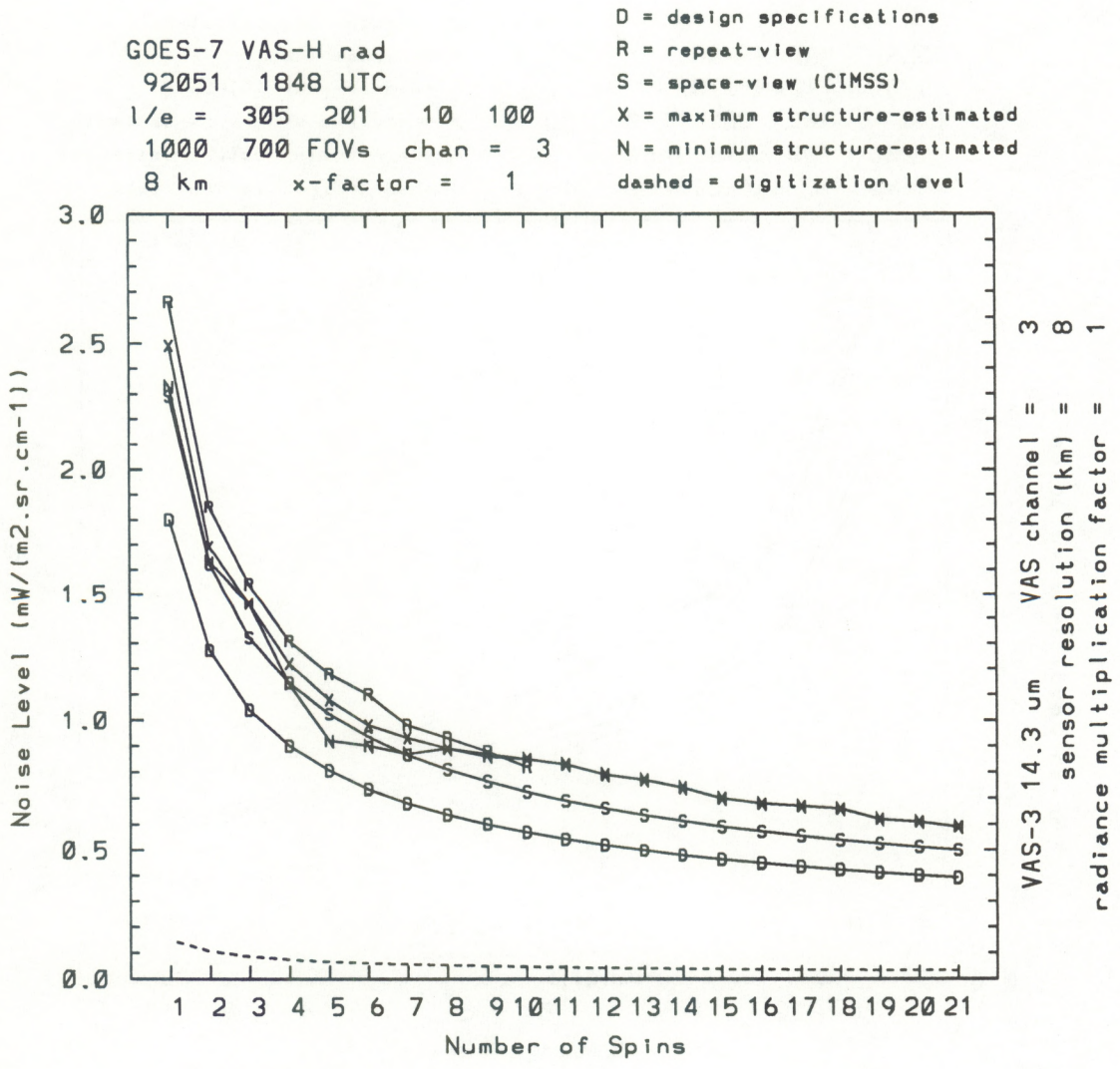

Figure 6c: Same as Figure 6a, but for VAS channel 3.

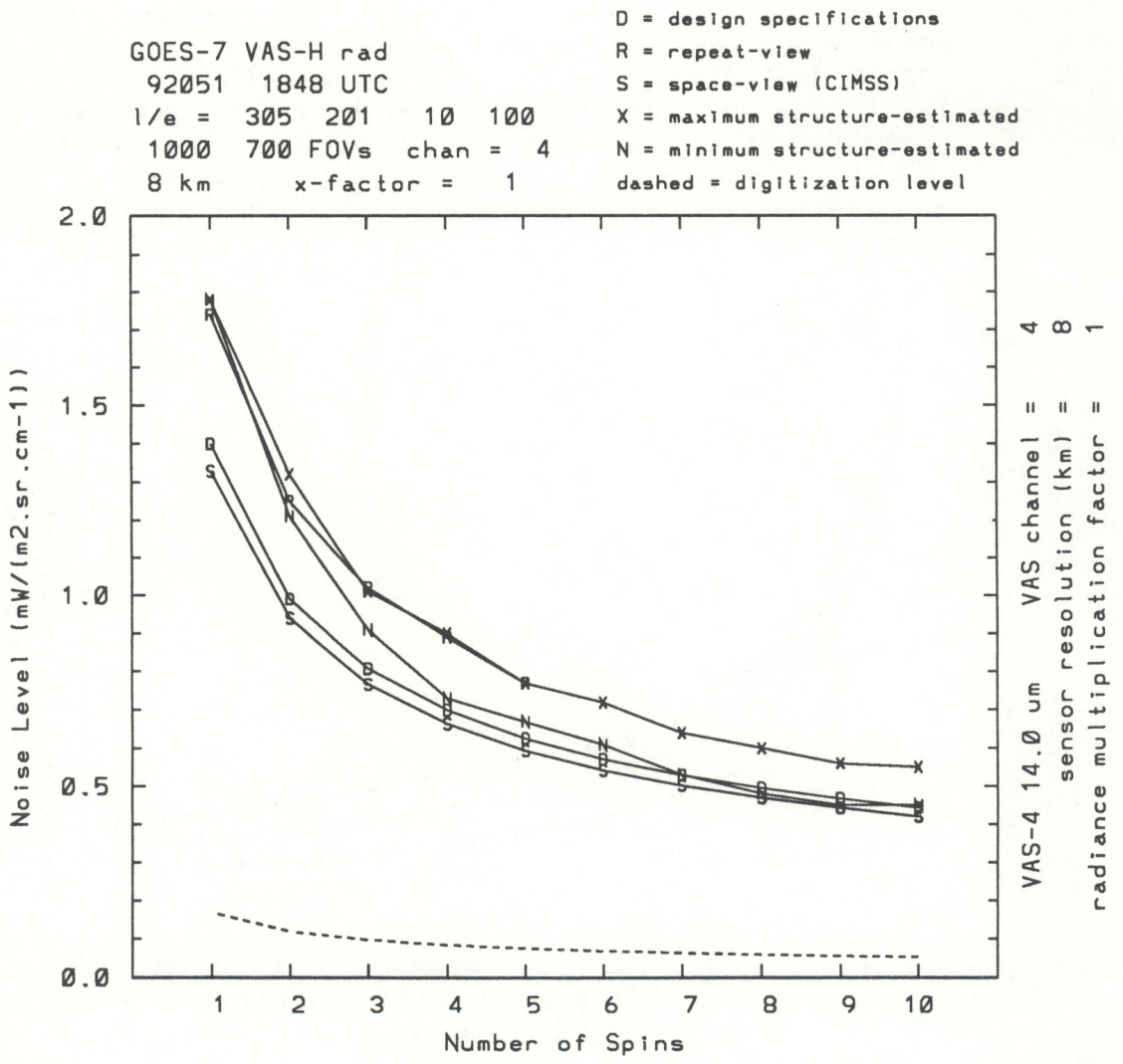

Figure 6d: Same as Figure 6a, but for VAS channel 4.

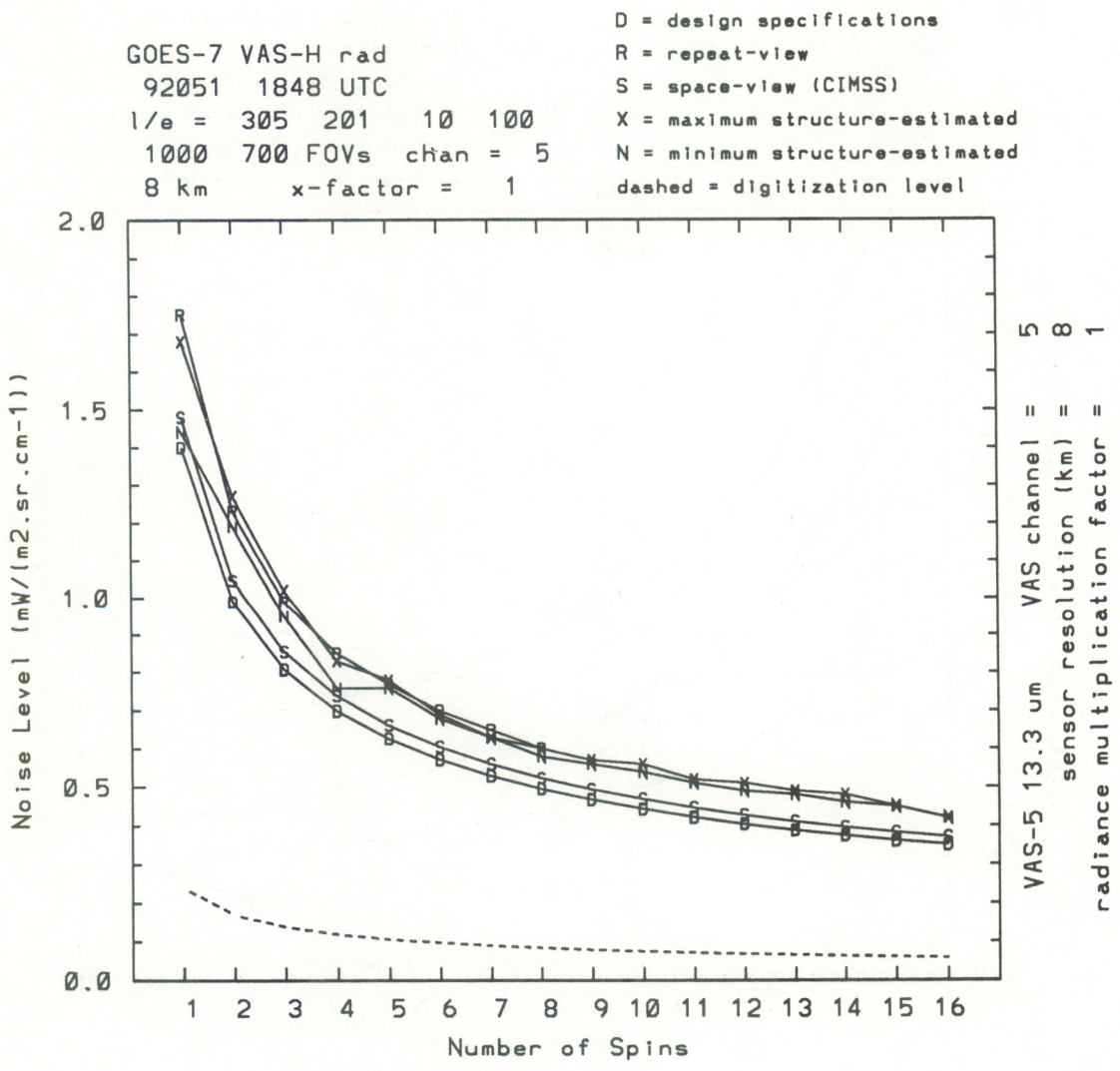

Figure 6e: Same as Figure 6a, but for VAS channel 5.

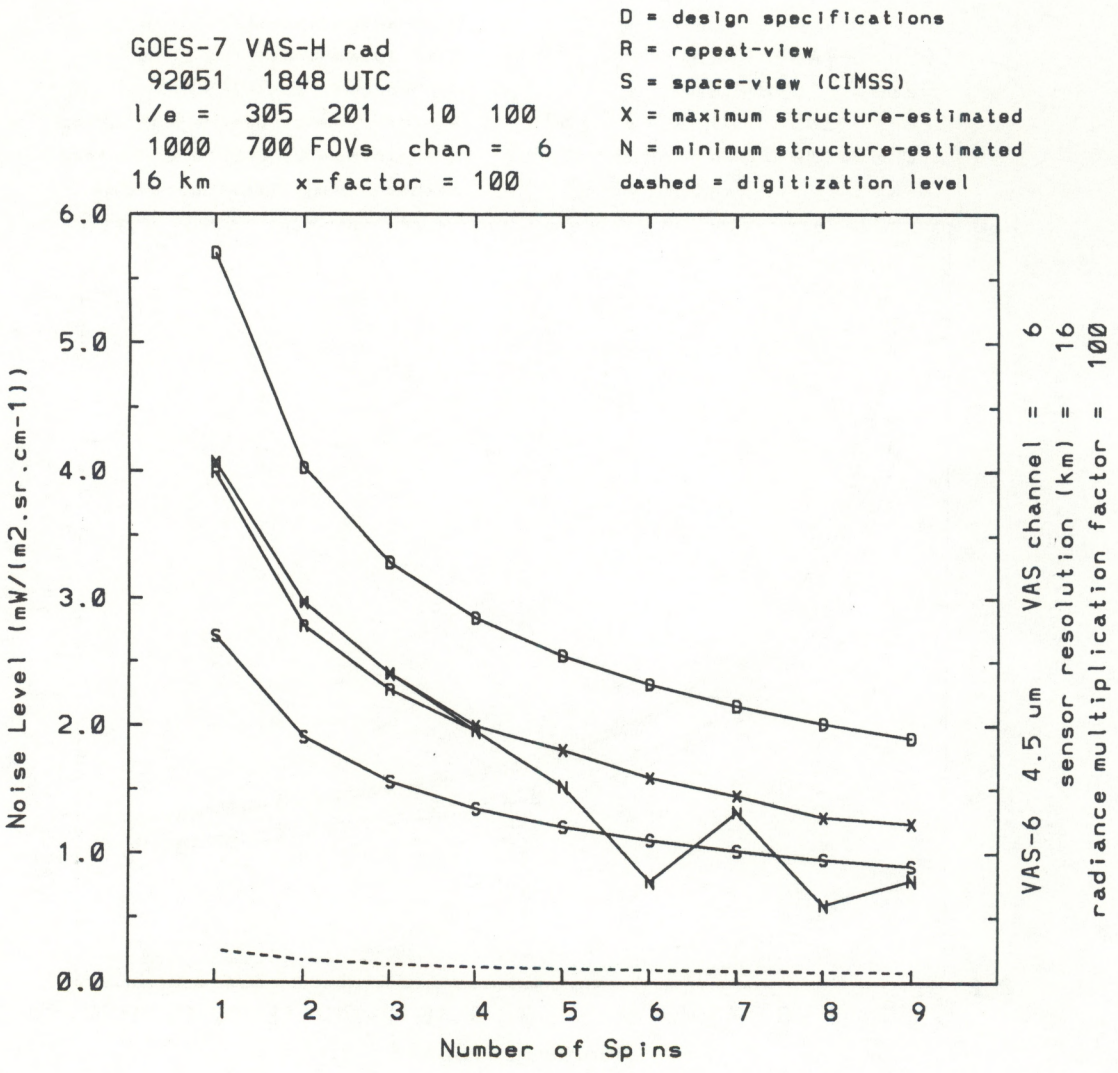

Figure 6f: Same as Figure 6a, but for VAS channel 6.

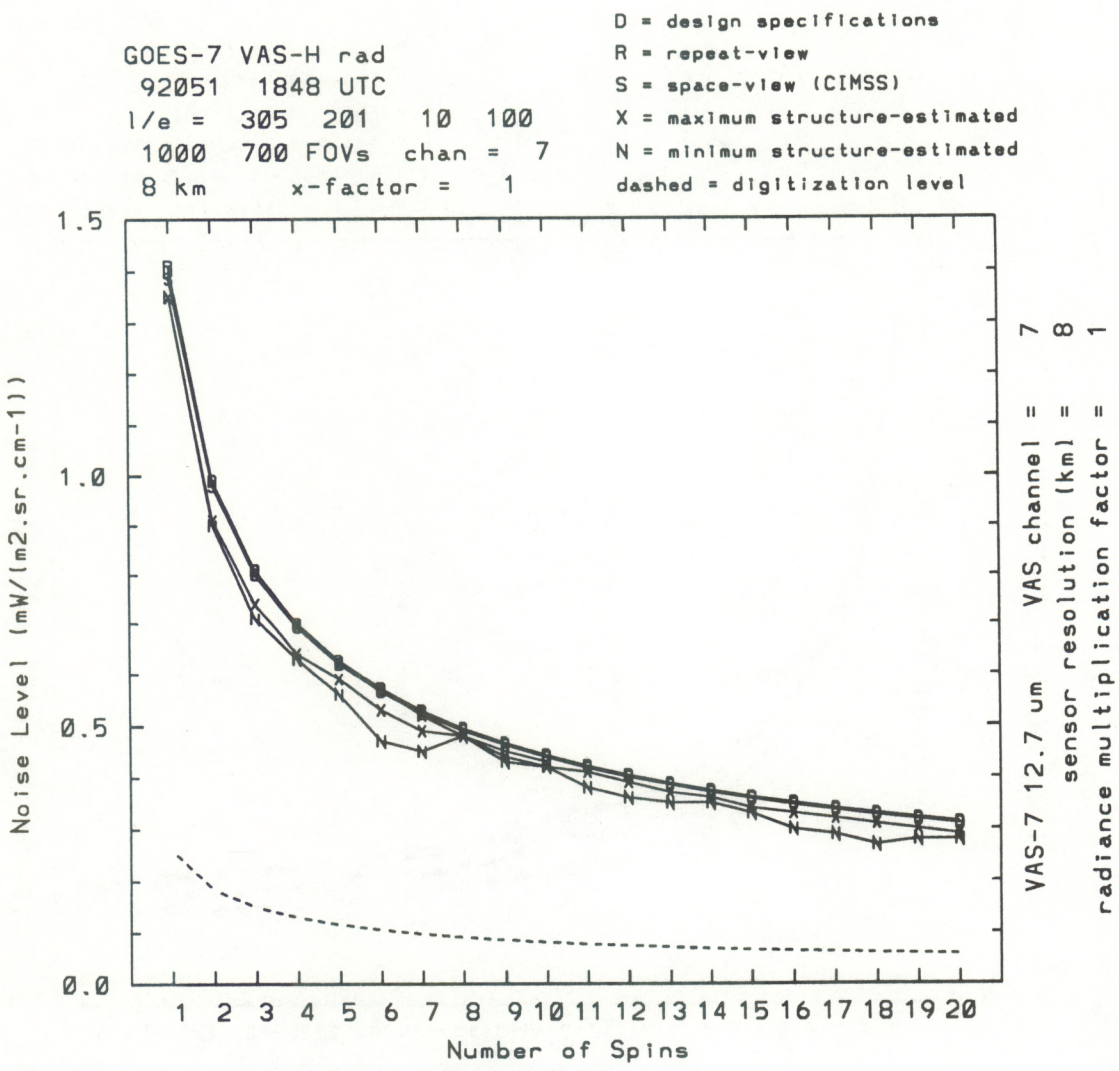

Figure 6g: Same as Figure 6a, but for VAS channel 7.

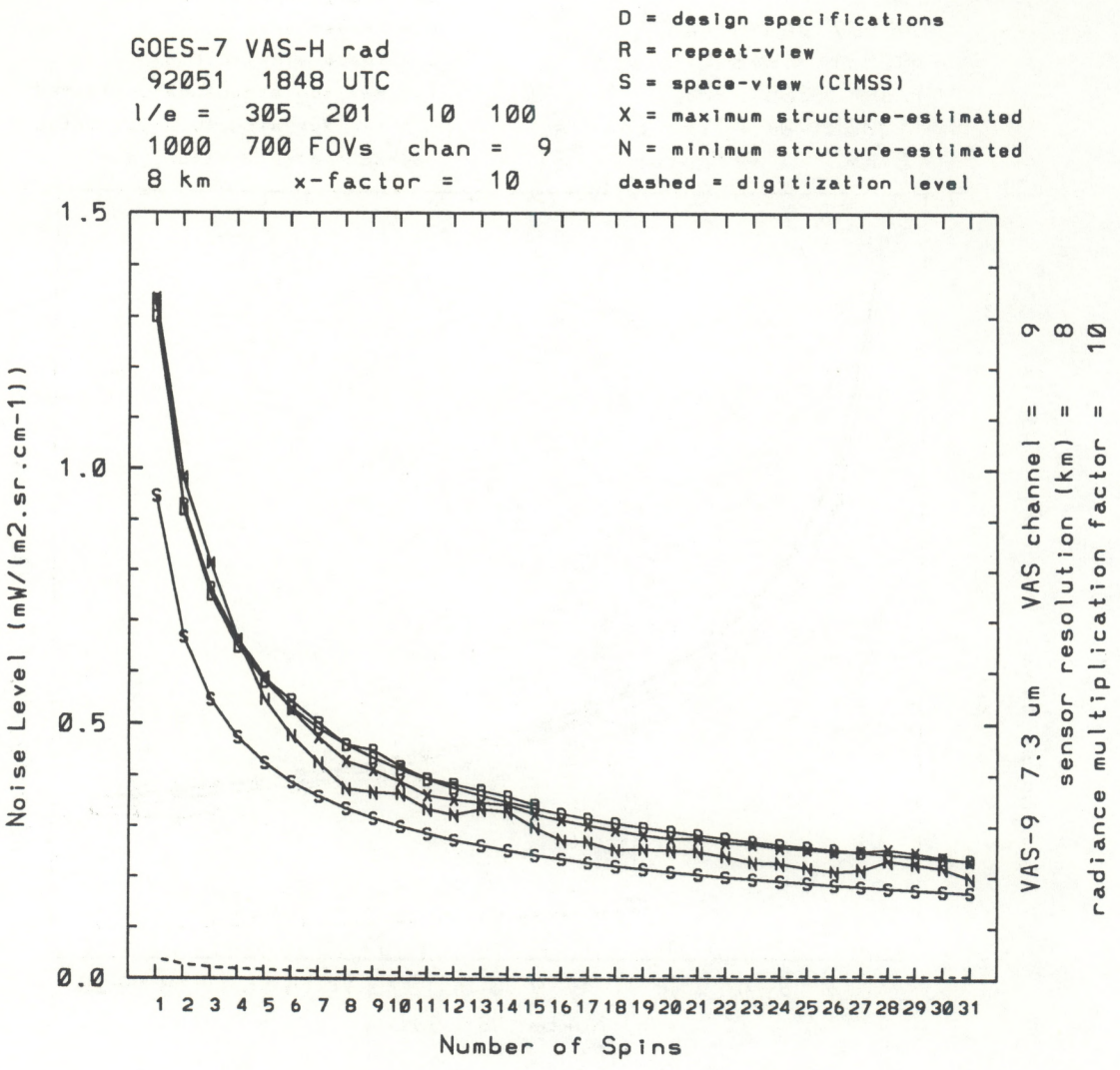

Figure 6h: Same as Figure 6a, but for VAS channel 9.

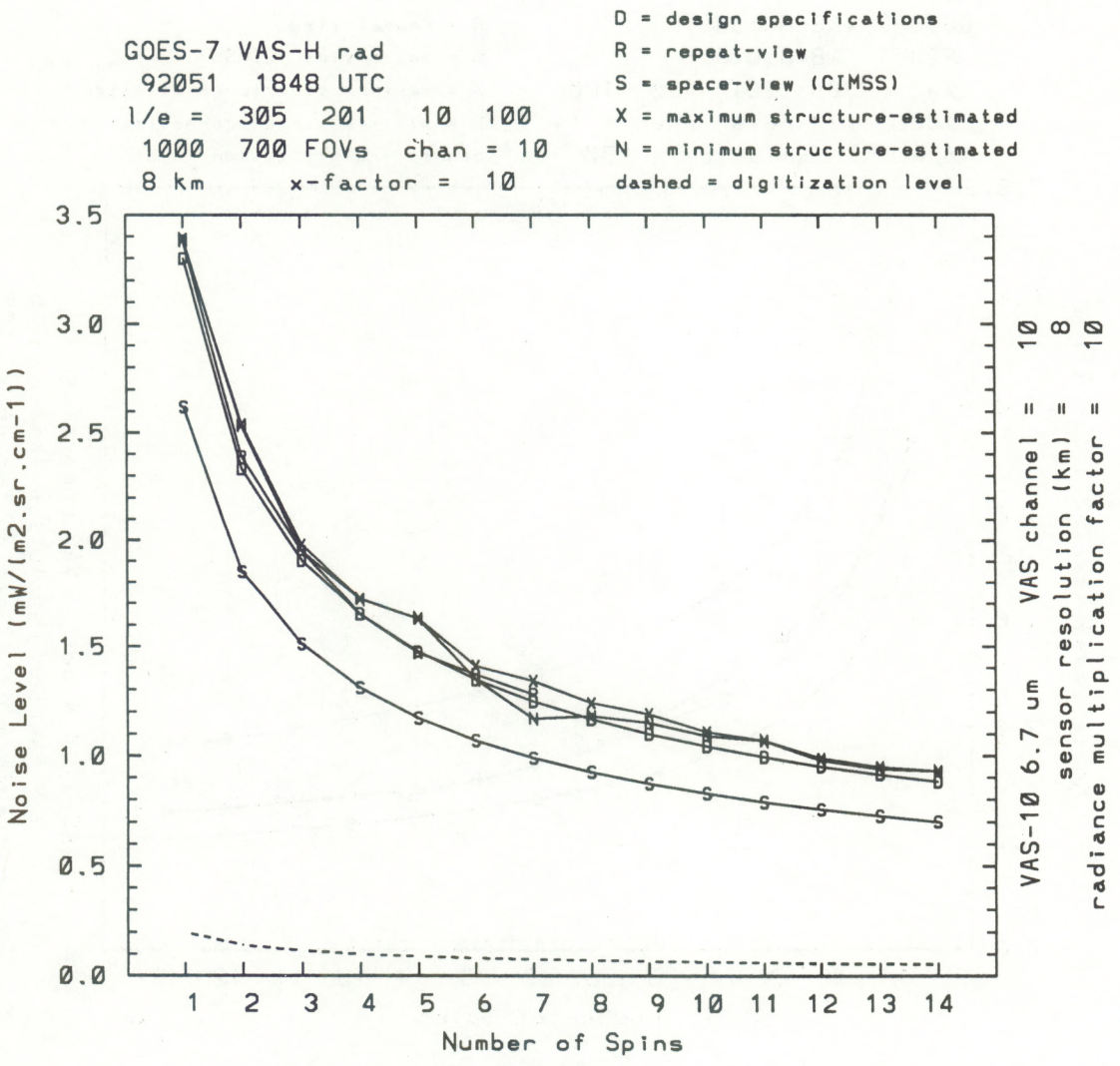

Figure 6i: Same as Figure 6a, but for VAS channel 10.

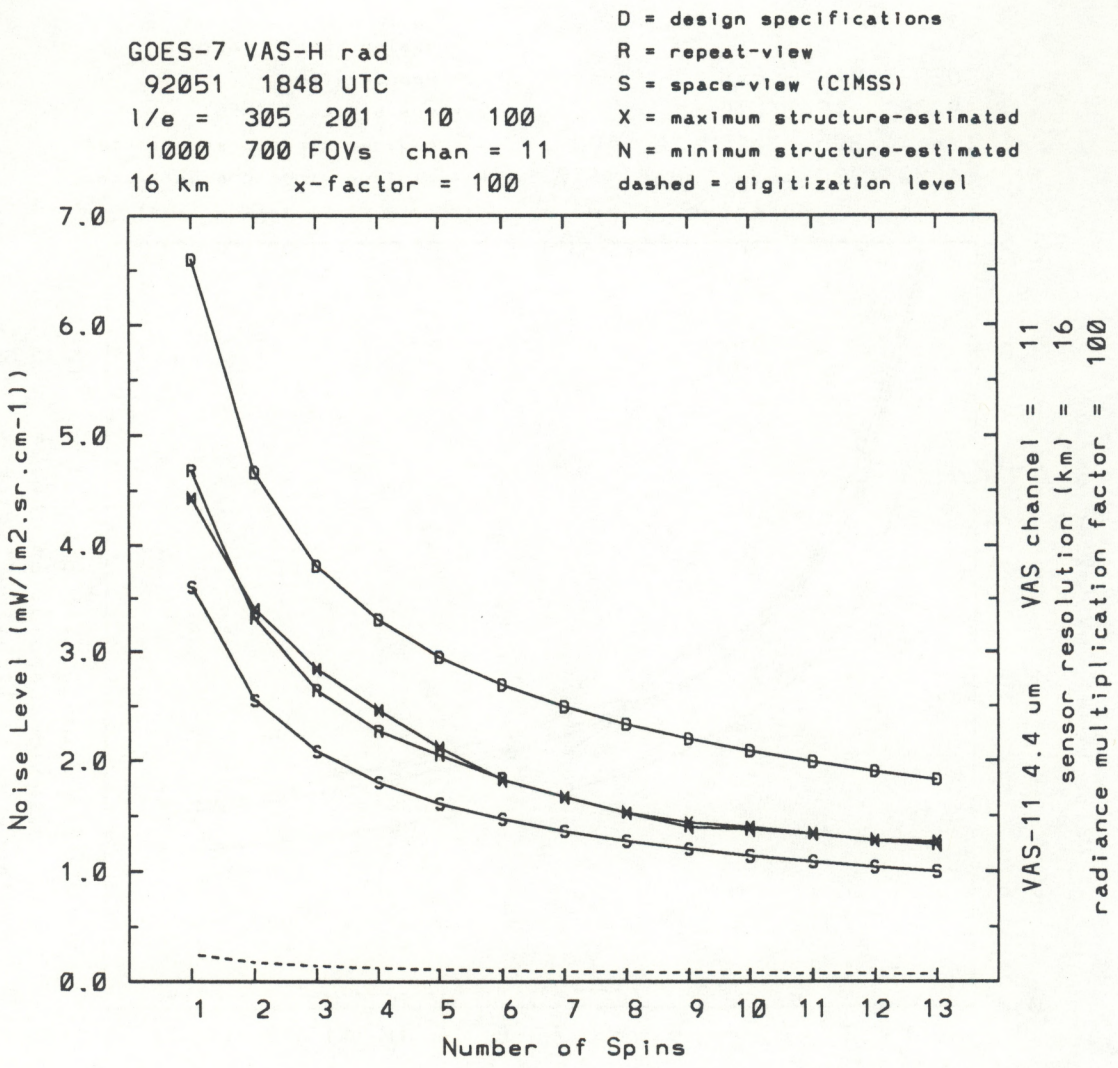

Figure 6j: Same as Figure 6a, but for VAS channel 11.

Table 6

Diurnal Variability
Date: 1992-March-06/07 (Julian-day 66/67)

VAS Channel	Mult-Factor	Mean (mW/...)	Standard Deviation (mW/...)	Percent
1	1	4.698	0.092	1.97
2	1	2.219	0.049	2.23
3	1	2.576	0.025	0.95
4	1	1.693	0.029	1.73
5	1	1.686	0.026	1.55
6	100	3.833	0.057	1.49
7	1	1.387	0.026	1.88
8	1	0.117	0.013	10.85
9	10	13.054	0.136	1.04
10	10	3.334	0.051	1.52
11	100	4.369	0.076	1.75
12	100	0.968	0.038	3.89

radiance units (mW/[m^2 sr cm^{-1}])

The results for VAS channel 6 are shown in Figure 7. The plot is formatted similar to the repeat-view noise level plot in Figure 4, but with time variation instead of spin variation. Results for all VAS channels show no detectable diurnal variation in noise off the edge of the earth, even though there may be a diurnal variation in the signal from the earth. This diurnal variation in the earth signal is apparent in the near infrared in VAS channel 6, but is most apparent in VAS channel 12 (not shown). The maximum signal occurs around 1750 UTC (local noon) with lower signals at night in the view of the satellite. The detection of no diurnal variation in noise agrees with the conclusions of Schmit and Menzel (1992) and Schmit (1992) showing no diurnal trend in their analyses of VAS noise levels.

8.0 SUMMARY AND CONCLUSIONS

Special high-spin-budget VAS data were collected during STORM-FEST from February through mid-March 1992. VAS radiances from off the edge of the earth were analyzed by three noise level estimation methods. Structure function analysis of adjacent FOVs was used to statistically determine the noise levels of multi-spin VAS data. Repeat-view analysis was used to statistically determine noise levels from single-spin VAS data through special data collection software capable of saving all the individual spins of VAS data. These noise level results were then compared to space-look results from CIMSS and to design specifications for the VAS instrument.

Results of the structure-estimated and the repeat-view methods were very similar for all VAS channels. This testifies to the reliability of the structure function method for determining noise levels, except for some cases of extrapolated noise levels. The repeat-view method is much simpler to perform, but only if multiple VAS measurements are saved at each FOV. Only when these multiple measurements are saved are comparisons of single-sample (1-spin) to multiple-sample noise levels possible.

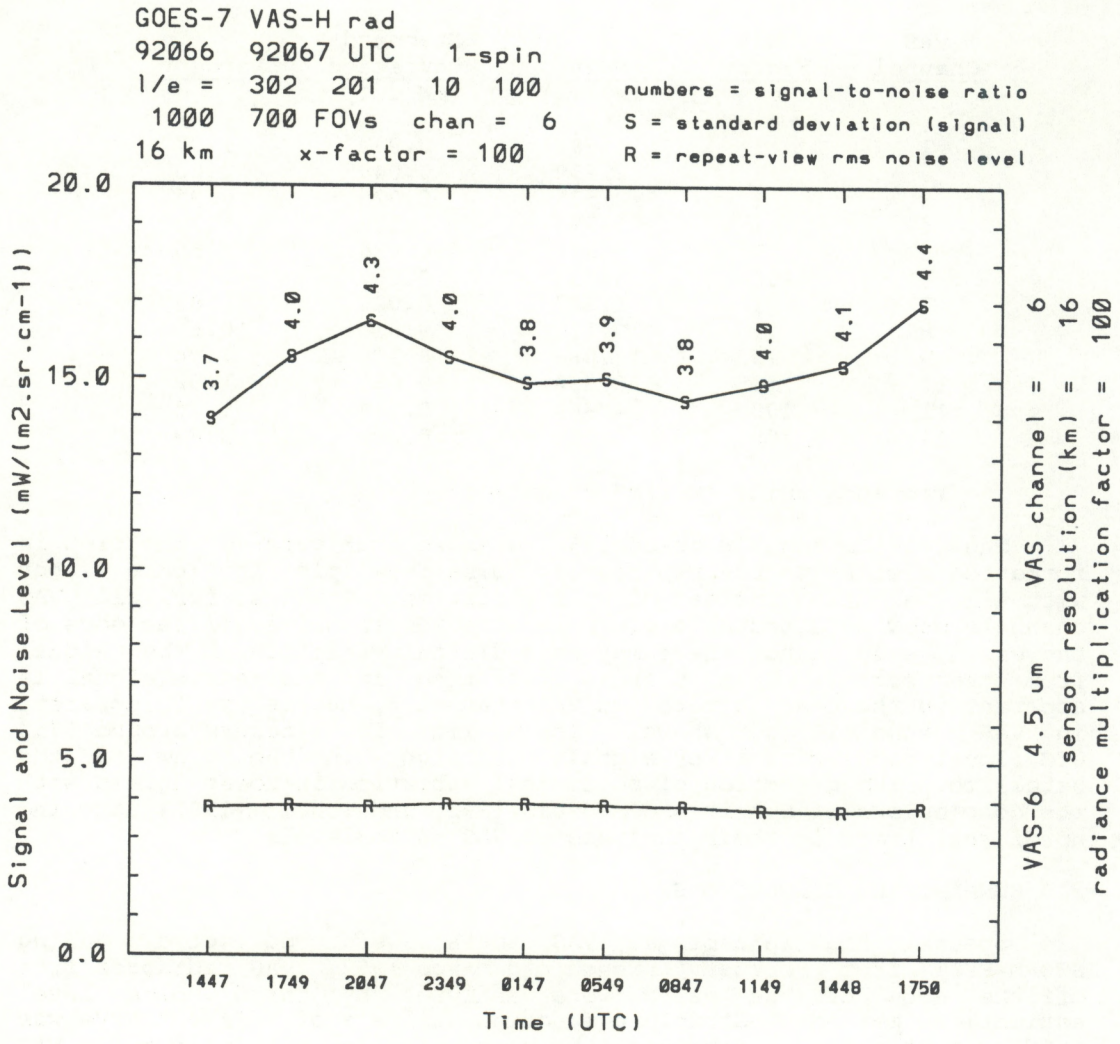

Figure 7: Noise levels for VAS channel 6 as a function of time. The analysis was performed every 3 hours from 1447 UTC on Julian-day 66 to 1750 UTC on Julian-day 67. Data times are spaced evenly except for 0147 UTC because data for 0247 UTC were corrupted in our data collection. Both signal 'S' and repeat-view 'R' noise level lines are shown, as well as dimensionless signal-to-noise ratios above the signal line.

Larger differences between the above two methods and the space-look noise levels provided by CIMSS are of more concern. The resulting noise level discrepancies may by due to inclusion of correlated VAS data in the sample. On the other hand, these discrepancies may indicate that multiple-spin space-look measurements should not be used alone to predict the noise level of VAS measurements. Single-spin VAS data can be used to verify the results of multiple-spin noise-level methods. Thus, occasional comparisons of the three methods would be wise.

The final analysis was to determine if there was any detectable diurnal variability in the VAS noise levels. Using data every 3 hours for a 30 hour period, the noise levels were determined, but the noise level variability was only a few percent of the mean noise level for all but VAS channel 8. Plots of the noise level with time showed no apparent diurnal trend in the noise for any of the VAS channels.

The determination of noise levels has many implications in conjunction with the spatial variability that can be measured at various wavelengths. One important application of such information could be to determine sensor effective spatial resolution for future satellites. Therefore, this study has implications for GOES-Next, which will include many channels similar to those on the present GOES. GOES-Next will not use multiple samples of the same FOVs to decrease noise levels, but the dwell time may be increased to decrease noise levels. The decrease in noise level with increasing dwell time should be tested using some of the first data collected from GOES-Next.

ACKNOWLEDGEMENTS

The authors thank T.J. Schmit and W.P. Menzel of NESDIS/CIMSS for the space-look noise levels used for comparison to the results of this study. Both Mr. Schmit and Dr. Menzel provided valuable feedback on the results presented in this report. A review of the manuscript was provided by Dr. S.B. Smith and Dr. P.M. Gabriel. This work was supported by NOAA Grant NA85RAH05045.

REFERENCES

Chesters,D., and W.D.Robinson, 1983: Performance appraisal of VAS radiometry for GOES-4, -5 and -6. NASA Technical Memorandum 85125, NASA/GSFC, 55-p.

Chesters,D., W.P.Menzel, H.E.Montgomery, and W.D.Robinson, 1985: VAS instrument performance appraisal. [in VAS Demonstration: (VISSR Atmospheric Sounder) Description and Final Report. NASA Reference Publication 1151.], NASA/GSFC, 17-33.

Gabriel,P.J., and J.F.W.Purdom, 1990a: Deconvolution of GOES infrared data. Fifth Conference on Satellite Meteorology and Oceanography, AMS, 3-7 September, London, UK, 181-184.

Gabriel,P.J., and J.F.W.Purdom, 1990b: Deconvolution of GOES infrared data. CIRA Newsletter, 5, Spring, 1-8.

Gandin,L.S., 1963: Objective Analysis of Meterological Fields. Translated from Russian, Israel Program for Scientific Translation, Jerusalem, 242-p. [NTIS: TT-65-50007]

Gomis,D., and S.Alonso, 1988: Structure function responses in a limited area. Mon. Wea. Rev., 116, 2254-2264.

Hillger,D.W. J.F.W.Purdom, and D.A.Lubich, 1991: A noise level analysis of special 10-spin-per-channel VAS data. NOAA Technical Report NESDIS 56, (February), 50-p.

Hillger,D.W., and T.H.Vonder Haar, 1979: An analysis of satellite infrared soundings at the mesoscale using statistical structure and correlation functions. J. Atmos. Sci., 36, 287-305.

Hillger,D.W., and T.H.Vonder Haar, 1988: Estimating noise levels of remotely-sensed measurements from satellites using spatial structure analysis. J. Atmos. Ocean. Tech., 5, 206-214.

Menzel,W.P., 1980: Pre-launch study report of VAS-D performance, Cooperative Institute for Meterological Satellite Studies, NASA Contract Report NAS5-21965, NASA/GSFC, 65-p.

Schmit,T.J., 1992: Personal communication.

Schmit,T.J., 1993: Personal communication.

Schmit,T.J., and W.P.Menzel, 1992: GOES/VAS infrared calibration, Infrared Radiometric Sensor Calibration Symposium, Logan,UT, (September 16), 20-p.

Wald,L., 1989: Some examples of the use of structure functions in the analysis of satellite images of the ocean. Photogrammetric Engineering and Remote Sensing, 55, 1487-1490.

(continued from inside cover)

NESDIS 31 Data Processing Alogorithms for Inferring Stratospheric Gas Concentrations from Balloon-Based Solar Occultation Data. I-Lok Chang (American University) and Michael P. Weinreb, April 1987. (PB87 196424)

NESDIS 32 Precipitation Detection with Satellite Microwave Data. Yang Chenggang and Andrew Timchalk, June 1988. (PB88 240239)

NESDIS 33 An Introduction to the GOES I-M Imager and Sounder Instruments and the GVAR Retransmission Format. Raymond J. Komajda (Mitre Corp) and Keith McKenzie, October 1987. (PB88 132709)

NESDIS 34 Balloon-Based Infrared Solar Occultation Measurements of Stratospheric 03, H20, HNo3, and CF2C12. Michael P. Weinreb and I-Lok Chang (American University), September 1987. (PB88 132725)

NESDIS 35 Passive Microwave Observing From Environmental Satellites, A Status Report Based on NOAA's June 1-4, 1987, Conference in Williamsburg, VA. James C. Fisher, November 1987. (PB88 208236)

NESDIS 36 Pre-Launch Calibration of Channels 1 and 2 of the Advanced Very High Resolution Radiometer. C. R. Nagaraja Rao, October 1987. (PB88 157169/AS)

NESDIS 39 General Determination of Earth Surface Type and Cloud Amount Using Multispectral AVHRR Data. Irwin Ruff and Arnold Gruber, February 1988. (PB88 199195/AS)

NESDIS 40 The GOES I-M System Functional Description. Carolyn Bradley (Mitre Corp), November 1988.

NESDIS 41 Report of the Earth Radiation Budget Requirements Review - 1987, Rosslyn, VA, 30 March-3 April 1987. Larry L. Stowe (Editor), June 1988.

NESDIS 42 Simulation Studies of Improved Sounding Systems. H. Yates, D. Wark, H. Aumann, N. Evans, N. Phillips, J. Sussking, L. McMillin, A. Goldman, M. Chahine and L. Crone, February 1989.

NESDIS 43 Adjustment of Microwave Spectral Radiances of the Earth to a Fixed Angle of Progagation. D. Q. Wark, December 1988. (PB89 162556/AS)

NESDIS 44 Educator's Guide for Building and Operating Environmental Satellite Receiving Stations. R. Joe Summers, Chambersburg Senior High, February 1989.

NESDIS 45 Final Report on the Modulation and EMC Consideration for the HRPT Transmission System in the Post NOAA-M Polar Orbiting Satellite ERA. James C. Fisher (Editor), June 1989. (PB89 223812/AS)

NESDIS 46 MECCA Program Documentation. Kurt W. Hess, September 1989.

NESDIS 47 A General Method of Using Prior Information in a Simultaneous Equation System. Lawrence J. Crone, David S. Crosby and Larry M. McMillin, October 1989.

NESDIS 49 Implementation of Reflectance Models in Operatioal AVHRR Radiation Budget Processing. V. Ray Taylor, February 1990.

NESDIS 50 A Comparison of ERBE and AVHRR Longwave Flux Estimates. A. Gruber, R. Ellingson, P. Ardanuy, M. Weiss, S. K. Yang, (Contributor: S.N. Oh).

NESDIS 51 The Impact of NOAA Satellite Soundings on the Numerical Analysis and Forecast System of the People's Republic of China. A. Gruber and W. Zonghao, May 1990.

NESDIS 52 Baseline Upper Air Network (BUAN) Final Report. A. L. Reale, H. E. Fleming, D. Q. Wark, C. S. Novak, F. S. Zbar, J. R. Neilon, M. E. Gelman and H. J. Bloom, October 1990.

NESDIS 53 NOAA-9 Solar Backscatter Ultraviolet (SBUV/2) Instrument and Derived Ozone Data: A Status Report Based on a Review on January 29, 1990. Walter G. Planet, June 1990.

NESDIS 54 Evaluation of Data Reduction and Compositing of the NOAA Global Vegetation Index Product: A Case Study. K. P. Gallo and J. F. Brown, July 1990.

NESDIS 55 Report of the Workshop on Radiometric Calibration of Satellite Sensors of Reflected Solar Radiation, March 27-28, 1990, Camp Springs, MD. Peter Abel (Editor), July 1990.

NESDIS 56 A Noise Level Analysis of Special 10-Spin-Per-Channel VAS Data. Donald W. Hillger, James F. W. Purdom and Debra A. Lubich, February 1991.

NESDIS 57 Water Vapor Imagery Interpretation and Applictions to Weather Analyis and Forecasting. Roger B. Weldon and Susan J. Holmes, April 1991.

NESDIS 58 Evaluating the Design of Satellite Scanning Radiometers for Earth Radiation Budget Measurements with System, Simulations. Part 1: Instantaneous Estimates. Larry Stowe, Philip Ardanuy, Richard Hucek, Peter Abel and Herberet Jacobowitz, October 1991.

NESDIS 59 Interactive Digital Image Display and Analysis System (IDIDAS) User's Guide. Peter J. Celone and William Y. Tseng, October 1991.

NESDIS 60 International Dobson Data Workshop Summary Report. Robert D. Hudson (University of Maryland) and Walter G. Planet, February 1992.

NESDIS 61 Tropical Cyclogenesis in the Western North Pacific. Raymond M. Zehr, July 1992.

NESDIS 62 NOAA Workshop on Climate Scale Operational Precipitation and Water Vapor Products. Ralph Ferraro (Editor), October 1992.

NOAA SCIENTIFIC AND TECHNICAL PUBLICATIONS

The National Oceanic and Atmospheric Administration was established as part of the Department of Commerce on October 3, 1970. The mission responsibilities of NOAA are to assess the socioeconomic impact of natural and technological changes in the environment and to monitor and predict the state of the solid Earth, the oceans and their living resources, the atmosphere, and the space environment of the Earth.

The major components of NOAA regularly produce various types of scientific and technical information in the following kinds of publications:

PROFESSIONAL PAPERS - Important definitive research results, major techniques, and special investigations.

CONTRACT AND GRANT REPORTS - Reports prepared by contractors or grantees under NOAA sponsorship.

ATLAS - Presentation of analyzed data generally in the form of maps showing distribution of rainfall, chemical and physical conditions of oceans and atmosphere, distribution of fishes and marine mammals, ionospheric conditions, etc.

TECHNICAL SERVICE PUBLICATIONS - Reports containing data, observations, instructions, etc. A partial listing includes data serials; prediction and outlook periodicals; technical manuals, training papers, planning reports, and information serials; and miscellaneous technical publications.

TECHNICAL REPORTS - Journal quality with extensive details, mathematical developments, or data listings.

TECHNICAL MEMORANDUMS - Reports of preliminary, partial, or negative research or technology results, interim instructions, and the like.

U.S. DEPARTMENT OF COMMERCE
National Oceanic and Atmospheric Administration
National Environmental Satellite, Data, and Information Service
Washington, D.C. 20233